

Integral Equations in Acoustics

TABLE OF CONTENTS

Table of Contents	1
1 Background Equation Chapter 1 Section 1	3
1.1 Green's Theorem	4
2 Volume Integral Equations Equation Section (Next)	5
2.1 Formulation	5
2.2 Define fields	7
2.3 Boundary Conditions	8
2.3.1 Sound-Soft (Dirichlet)	8
2.3.2 Sound-Hard (Neumann)	8
2.3.3 Sound-Soft Combined Field Integral Equation (CFIE)	11
2.3.4 Sound-Hard Combined Field Integral Equation (CFIE)	13
3 Method of Moments	15
3.1 Sound-soft	15
3.2 Sound-Soft CFIE	16
3.3 Numerical Integration	17
3.3.1 Gaussian Quadrature	17
3.4 Integration Routines	19
4 Scattering Matrix	21
4.1.1 Acoustic Derivation	21
4.1.2 Scattering Matrix Implementation	23
5 Wigner-Smith Equation Section (Next)	27
5.1 Introduction	27
5.2 Derivation of Q	27
5.2.1 One-port System	27
5.2.2 Multi-port System	29
5.3 WS Modes	31
5.3.1 Properties of Q	31
5.3.2 What does Q represent?	32
5.3.3 Fields of WS Modes	32
5.3.4 WS and Method of Moments	33

6	Adaptive Cross Approximation	34
6.1	Algorithm.....	34
6.2	Metrics	34
7	Appendix Equation Section (Next)	36
7.1	Linear Algebra	36
7.1.1	Matrix Diagonalization	36
8	References.....	37

1 INTRODUCTION

This document describes the mathematical underpinnings of an associated integral equation based acoustic scattering simulation developed by Jack Hamel at the University of Michigan – Ann Arbor. The code is capable of computing the equivalent surface sources on an arbitrary scatterer's surface due to an arbitrary plane wave or spherical wave impinging on the surface. The user has the option of solving a variety of integral equation formulations to this end as well as using an accelerated solver routine based on the adaptive cross approximation. In addition, the code can compute the Wigner-Smith matrix and ultimately the time delays for each Wigner-Smith mode of the scatterer as well as simulate the scatter when excited by an incident wave that exactly induces any desired Wigner-Smith mode.

This document attempts to be comprehensive though details of some algorithms such as singular integration and the adaptive cross approximation are omitted and the sources exactly describing the implementations in the code are referenced. This document does not directly reference the associated code at this time. Also, please be aware that two different equation editors were used in writing this document and that causes out-of-order and duplicate reference numbers for equations that can lead to confusion. Lastly, there are currently no in-text citations right now. There is an intention to fix these issues at some point.

2 BACKGROUND EQUATION CHAPTER 1 SECTION 1

2.1 GREEN'S THEOREM

Start by applying divergence theorem over a volume V circumscribed by closed-surface S to $\psi \nabla \phi$, where ψ and ϕ are scalar functions of position with continuous first and second derivatives in V and on S .

$$\iiint_V \nabla \cdot (\psi \nabla \phi) dV = \oiint_S (\psi \nabla \phi) \cdot d\mathbf{s}$$

Recall that $\nabla \phi \cdot \hat{\mathbf{n}} = \frac{\partial \phi}{\partial n}$, where $\hat{\mathbf{n}}$ is the outward pointing normal unit vector on S , and the vector identity $\nabla \cdot (\psi \nabla \phi) = \psi \nabla^2 \phi + \nabla \psi \cdot \nabla \phi$ and the above equation becomes

$$\iiint_V (\psi \nabla^2 \phi + \nabla \psi \cdot \nabla \phi) dV = \oiint_S \psi \frac{\partial \phi}{\partial n} dS \quad (1.1)$$

Equation (1.1) is known as Green's first identity.

To derive Green's second identity (a.k.a Green's Theorem), start by interchanging ψ and ϕ in (1.1).

$$\iiint_V (\phi \nabla^2 \psi + \nabla \phi \cdot \nabla \psi) dV = \oiint_S \phi \frac{\partial \psi}{\partial n} dS$$

Subtracting the above equation from (1.1) yields Green's Theorem.

$$\iiint_V (\psi \nabla^2 \phi - \phi \nabla^2 \psi) dV = \oiint_S \left(\psi \frac{\partial \phi}{\partial n} - \phi \frac{\partial \psi}{\partial n} \right) dS \quad (1.2)$$

3 VOLUME INTEGRAL EQUATIONS EQUATION SECTION (NEXT)

3.1 FORMULATION

In the region depicted in Figure 1 the scalar fields, $\phi^{\text{inc}}(\mathbf{r})$, $\phi^{\text{sca}}(\mathbf{r})$ and $G(\mathbf{r}, \mathbf{r}')$ obey the 3D inhomogeneous wave equations

$$\begin{aligned}\nabla^2 \phi^{\text{sca}}(\mathbf{r}) + k^2 \phi^{\text{sca}}(\mathbf{r}) &= -\delta(\mathbf{r} - \mathbf{r}^s) \\ \nabla^2 \phi^{\text{inc}}(\mathbf{r}) + k^2 \phi^{\text{inc}}(\mathbf{r}) &= -\delta(\mathbf{r} - \mathbf{r}^i) \\ \nabla^2 G(\mathbf{r}, \mathbf{r}') + k^2 G(\mathbf{r}, \mathbf{r}') &= -\delta(\mathbf{r} - \mathbf{r}')\end{aligned}\tag{2.1}$$

Where $G(\mathbf{r}, \mathbf{r}') = \frac{e^{-jk|\mathbf{r}-\mathbf{r}'|}}{4\pi|\mathbf{r}-\mathbf{r}'|}$ is the scalar Green's function and \mathbf{r} , \mathbf{r}' , \mathbf{r}^s and \mathbf{r}^i are the position vectors

for the observation point, equivalent sources, scatterer sources and incident field sources respectively. It is obvious that $G(\mathbf{r}, \mathbf{r}') = G(\mathbf{r}', \mathbf{r})$, $\phi^{\text{inc}}(\mathbf{r}') = G(\mathbf{r}^i, \mathbf{r}')$ and $\phi^{\text{sca}}(\mathbf{r}') = G(\mathbf{r}^s, \mathbf{r}')$.

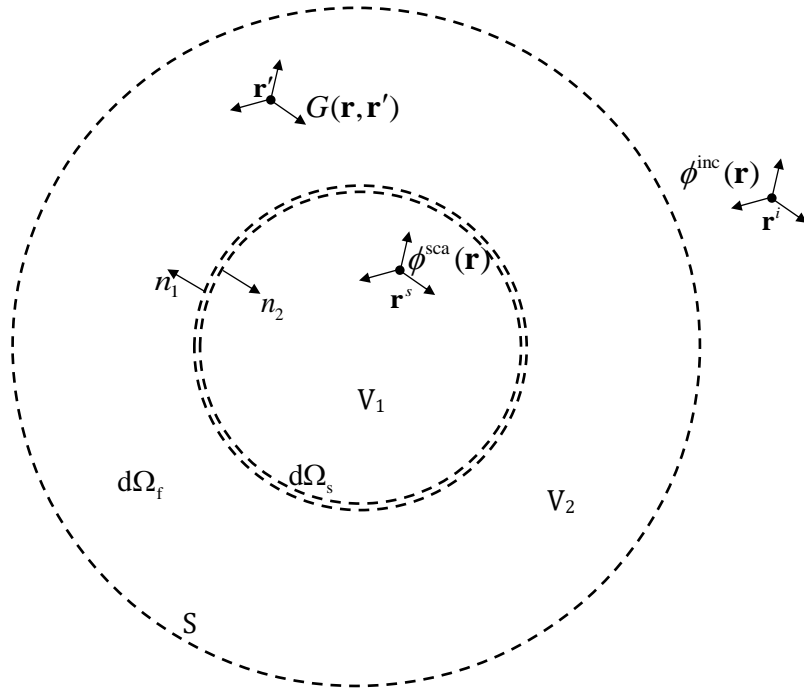


Figure 1: Volume V_1 with radius r_s is circumscribed by the surface S , sitting an infinitesimal distance above the scatterer whose surface is circumscribed by $d\Omega_s$. Volume V_2 is bounded by the surface

$d\Omega_f$ located at radius $r_f \gg r_s$.

Ignoring the scatterer, $d\Omega_s$, for the time being, and letting the scatterer be the delta function in equation (2.1), Green's Theorem can be applied over V_1 to $\phi^{\text{sca}}(\mathbf{r})$ and $G(\mathbf{r}, \mathbf{r}')$

$$\iiint_{V_1} (\phi^{\text{sca}}(\mathbf{r}) \nabla^2 G(\mathbf{r}, \mathbf{r}') - G(\mathbf{r}, \mathbf{r}') \nabla^2 \phi^{\text{sca}}(\mathbf{r})) dV = \oint\!\!\!\oint_S \left(\phi^{\text{sca}}(\mathbf{r}) \frac{\partial G(\mathbf{r}, \mathbf{r}')}{\partial n_1} - G(\mathbf{r}, \mathbf{r}') \frac{\partial \phi^{\text{sca}}(\mathbf{r})}{\partial n_1} \right) dS$$

Substituting in equations (2.1)

$$\iiint_{V_1} (-\phi^{\text{sca}}(\mathbf{r}) \delta(\mathbf{r} - \mathbf{r}') - G(\mathbf{r}, \mathbf{r}') \delta(\mathbf{r} - \mathbf{r}^s)) dV = \oint\!\!\!\oint_S \left(\phi^{\text{sca}}(\mathbf{r}) \frac{\partial G(\mathbf{r}, \mathbf{r}')}{\partial n_1} - G(\mathbf{r}, \mathbf{r}') \frac{\partial \phi^{\text{sca}}(\mathbf{r})}{\partial n_1} \right) dS \quad (2.2)$$

The LHS is piecewise depending on the locations of the sources

$$\iiint_{V_1} (-\phi^{\text{sca}}(\mathbf{r}) \delta(\mathbf{r} - \mathbf{r}') + G(\mathbf{r}, \mathbf{r}') \delta(\mathbf{r} - \mathbf{r}^s)) dV = \begin{cases} -\phi^{\text{sca}}(\mathbf{r}') + G(\mathbf{r}^s, \mathbf{r}') = 0, & \mathbf{r}^s, \mathbf{r}' \in V_1 \\ G(\mathbf{r}^s, \mathbf{r}'), & \mathbf{r}^s \in V_1, \mathbf{r}' \notin V_1 \\ -\phi^{\text{sca}}(\mathbf{r}'), & \mathbf{r}' \in V_1, \mathbf{r}^s \notin V_1 \\ 0, & \mathbf{r}^s, \mathbf{r}' \notin V_1 \end{cases}$$

Referencing the equation above, $\mathbf{r}^s \in V_1$ and $\mathbf{r}' \in V_2$ thus Green's theorem boils down to

$$G(\mathbf{r}^s, \mathbf{r}') = \phi^{\text{sca}}(\mathbf{r}') = \oint\!\!\!\oint_S \left(\phi^{\text{sca}}(\mathbf{r}) \frac{\partial G(\mathbf{r}, \mathbf{r}')}{\partial n_1} - G(\mathbf{r}, \mathbf{r}') \frac{\partial \phi^{\text{sca}}(\mathbf{r})}{\partial n_1} \right) dS \quad (2.3)$$

Green's theorem is now applied over V_1 to $\phi^{\text{inc}}(\mathbf{r})$ and $G(\mathbf{r}, \mathbf{r}')$

$$\iiint_{V_1} (\phi^{\text{inc}}(\mathbf{r}) \nabla^2 G(\mathbf{r}, \mathbf{r}') - G(\mathbf{r}, \mathbf{r}') \nabla^2 \phi^{\text{inc}}(\mathbf{r})) dV = \oint\!\!\!\oint_S \left(\phi^{\text{inc}}(\mathbf{r}) \frac{\partial G(\mathbf{r}, \mathbf{r}')}{\partial n_1} - G(\mathbf{r}, \mathbf{r}') \frac{\partial \phi^{\text{inc}}(\mathbf{r})}{\partial n_1} \right) dS$$

Substituting in equations (2.1), the LHS is piecewise depending on the source locations

$$\iiint_{V_1} (-\phi^{\text{inc}}(\mathbf{r}) \delta(\mathbf{r} - \mathbf{r}') + G(\mathbf{r}, \mathbf{r}') \delta(\mathbf{r} - \mathbf{r}^i)) dV = \begin{cases} -\phi^{\text{inc}}(\mathbf{r}') + G(\mathbf{r}^i, \mathbf{r}') = 0, & \mathbf{r}^i, \mathbf{r}' \in V_1 \\ G(\mathbf{r}^i, \mathbf{r}'), & \mathbf{r}^i \in V_1, \mathbf{r}' \notin V_1 \\ -\phi^{\text{inc}}(\mathbf{r}'), & \mathbf{r}' \in V_1, \mathbf{r}^i \notin V_1 \\ 0, & \mathbf{r}^i, \mathbf{r}' \notin V_1 \end{cases}$$

Referencing the figure, $\mathbf{r}^i \notin V_1$ and $\mathbf{r}' \notin V_1$

$$0 = \oint\!\!\!\oint_S \left(\phi^{\text{inc}}(\mathbf{r}) \frac{\partial G(\mathbf{r}, \mathbf{r}')}{\partial n_1} - G(\mathbf{r}, \mathbf{r}') \frac{\partial \phi^{\text{inc}}(\mathbf{r})}{\partial n_1} \right) dS \quad (2.4)$$

Define

$$\phi(\mathbf{r}) = \phi^{\text{sca}}(\mathbf{r}) + \phi^{\text{inc}}(\mathbf{r}) \quad (2.5)$$

Add equations (2.3) and (2.4) and apply a change of variable from $\mathbf{r} \leftrightarrow \mathbf{r}'$

$$\phi^{\text{sca}}(\mathbf{r}) = \oint\!\!\!\oint_S \left(\phi(\mathbf{r}') \frac{\partial G(\mathbf{r}, \mathbf{r}')}{\partial n'_1} - G(\mathbf{r}, \mathbf{r}') \frac{\partial \phi(\mathbf{r}')}{\partial n'_1} \right) dS' \quad (2.6)$$

Extinction Theorem

Note that if (after the change of variable) $\mathbf{r} \in V_1$ (i.e. the observation point is within S), then the LHS of equation (2.3) would become zero and the LHS of equation (2.4) would become $-\phi^{\text{inc}}(\mathbf{r}')$ and equation (2.6) would look like

$$0 = \phi^{\text{inc}}(\mathbf{r}) + \oint\!\!\!\oint_S \left(\phi(\mathbf{r}') \frac{\partial G(\mathbf{r}, \mathbf{r}')}{\partial n'_1} - G(\mathbf{r}, \mathbf{r}') \frac{\partial \phi(\mathbf{r}')}{\partial n'_1} \right) dS' \quad (2.7)$$

Meaning the surface sources in the integral term produce a field equal to the incident field inside V_1 therefore the total field inside V_1 is zero.

With extinction theorem, equation (2.6) can be interpreted as replacing the sources inside V_1 by surface sources $\phi(\mathbf{r}')$ and $-\frac{\partial \phi(\mathbf{r}')}{\partial n'_1}$ on S such that the fields in V_2 are maintained and the fields in V_1 are zero. In fact, this does not apply only to a single delta source in V_1 . Any arbitrary source sitting inside S can be treated as a sum of delta functions. Thus equation (2.6) is the volume integral equation for an arbitrary acoustic scatterer circumscribed by surface $d\Omega_s$ within V_1 .

3.2 DEFINE FIELDS

The incident field is further defined to be a spherical wave as follows

$$\begin{aligned} \phi_p^{\text{inc}}(\mathbf{r}) &= \mathcal{W}_p(kr) \\ &= 2kj_p(kr)Y_p(\theta, \phi) \\ &= k \left[h_p^{(1)}(kr) + h_p^{(2)}(kr) \right] Y_p(\theta, \phi) \\ &= \mathcal{I}_p(kr) + \mathcal{O}_p(kr) \end{aligned} \quad (2.8)$$

Where $\mathcal{I}_p(kr)$ and $\mathcal{O}_p(kr)$ are incoming and outgoing components, respectively, of the incident field.

Additionally, since $d\Omega_f$ is located at $r_f \gg r_s$, we can define far-field expressions for $\phi^{\text{sca}}(\mathbf{r})$ on it. Far-field expressions are denoted as $\phi_{p,\parallel}^{\text{sca}}(\mathbf{r})$ and are equivalent to their respective expressions with valid far-field approximations applied.

3.3 BOUNDARY CONDITIONS

By applying valid boundary conditions to the problem of the previous chapter, standard acoustical integral equations can be derived. At this point, it is worth clarifying that from Figure 1 the surface S sits an infinitesimal distance above the surface of the scatterer, $d\Omega_s$. This ensures the derivations of section 2.1 remain valid.

3.3.1 Sound-Soft (Dirichlet)

The sound-soft or Dirichlet, as known in mathematics, boundary condition on S is

$$\phi(\mathbf{r}) = \phi^{sca}(\mathbf{r}) + \phi^{inc}(\mathbf{r}) = 0 \quad \forall \mathbf{r} \in S$$

Under this condition, equation (2.6) reduces to

$$\phi^{sca}(\mathbf{r}) = \iint_S G(\mathbf{r}, \mathbf{r}') \left(-\frac{\partial \phi(\mathbf{r}')}{\partial n'_1} \right) dS'$$

$$\text{Let } \sigma(\mathbf{r}') = -\frac{\partial \phi(\mathbf{r}')}{\partial n'_1}$$

$$\phi^{sca}(\mathbf{r}) = \iint_S G(\mathbf{r}, \mathbf{r}') \sigma(\mathbf{r}') dS' \quad (3.1)$$

Restricting $\mathbf{r} \in S$ and relating scattered and incident fields

$$-\phi^{inc}(\mathbf{r}) = \iint_S G(\mathbf{r}, \mathbf{r}') \sigma(\mathbf{r}') dS' \quad (3.2)$$

$\sigma(\mathbf{r}')$ can be solved for using equation (3.2) and then the scattered fields can be calculated anywhere outside of V_1 .

Sound-Soft Normal Derivative Integral Equation

In electromagnetics, the above formulation would be known as the “Electric Field Integral Equation” and following from its derivation is the “Magnetic Field Integral Equation”. The same can be done in acoustics and will be referred to as the sound-soft normal derivative IE because it is obtained by taking the normal derivative of equation (3.1) using the normal vector of the scatterer’s surface located at \mathbf{r} .

$$\frac{\partial \phi^{sca}(\mathbf{r})}{\partial n_1} = \iint_S \frac{\partial G(\mathbf{r}, \mathbf{r}')}{\partial n_1} \sigma(\mathbf{r}') dS'$$

The integral above can be calculated in the principal value sense whereby the exclusion occurs when $\mathbf{r} = \mathbf{r}'$. It is shown in section 3.3.2 how to do this in more detail with the difference here being we are taking the derivative with respect to un-primed coordinates which introduces a negative sign in the results. Applying equation (3.4)

$$\frac{\partial \phi^{sca}(\mathbf{r})}{\partial n_1} = -\frac{\sigma(\mathbf{r})}{2} + \text{p.v.} \iint_S \frac{\partial G(\mathbf{r}, \mathbf{r}')}{\partial n_1} \sigma(\mathbf{r}') dS'$$

Applying the normal derivative to $\phi(\mathbf{r})$ when $\mathbf{r} \in S$

$$\frac{\partial \phi(\mathbf{r})}{\partial n_1} = \frac{\partial \phi^{inc}(\mathbf{r})}{\partial n_1} + \frac{\partial \phi^{sca}(\mathbf{r})}{\partial n_1} \Rightarrow \frac{\partial \phi^{sca}(\mathbf{r})}{\partial n_1} = -\sigma(\mathbf{r}) - \frac{\partial \phi^{inc}(\mathbf{r})}{\partial n_1}$$

And finally

$$\begin{aligned} -\sigma(\mathbf{r}) - \frac{\partial \phi^{inc}(\mathbf{r})}{\partial n_1} &= -\frac{\sigma(\mathbf{r})}{2} + \text{p.v.} \iint_S \frac{\partial G(\mathbf{r}, \mathbf{r}')}{\partial n_1} \sigma(\mathbf{r}') dS' \\ -\frac{\partial \phi^{inc}(\mathbf{r})}{\partial n_1} &= \frac{\sigma(\mathbf{r})}{2} + \text{p.v.} \iint_S \frac{\partial G(\mathbf{r}, \mathbf{r}')}{\partial n_1} \sigma(\mathbf{r}') dS' \end{aligned} \quad (3.3)$$

is the sound-soft normal derivative IE.

3.3.2 Sound-Hard (Neumann)

The sound-hard or Neumann, as known in mathematics, boundary condition on S is

$$\frac{\partial \phi(\mathbf{r})}{\partial n_1} = 0 \quad \forall \mathbf{r} \in S$$

Under this condition, equation (2.6) reduces to

$$\phi^{sca}(\mathbf{r}) = \iint_S \phi(\mathbf{r}') \frac{\partial G(\mathbf{r}, \mathbf{r}')}{\partial n'_1} dS'$$

Let $\sigma(\mathbf{r}') = \phi(\mathbf{r}')$

$$\phi^{sca}(\mathbf{r}) = \iint_S \sigma(\mathbf{r}') \frac{\partial G(\mathbf{r}, \mathbf{r}')}{\partial n'_1} dS'$$

Restricting $\mathbf{r} \in S$ and using equation (2.5)

$$-\phi^{inc}(\mathbf{r}) = -\sigma(\mathbf{r}) + \iint_S \frac{\partial G(\mathbf{r}, \mathbf{r}')}{\partial n'_1} \sigma(\mathbf{r}') dS' \quad (2.9)$$

Equation (2.9) is not as pleasant as the sound-soft integral equation because the RHS is discontinuous across the boundary S ($\nabla G(\mathbf{r}, \mathbf{r}')$ switches signs across S) as shown in the figure below. See appendix for more details on the discontinuity.

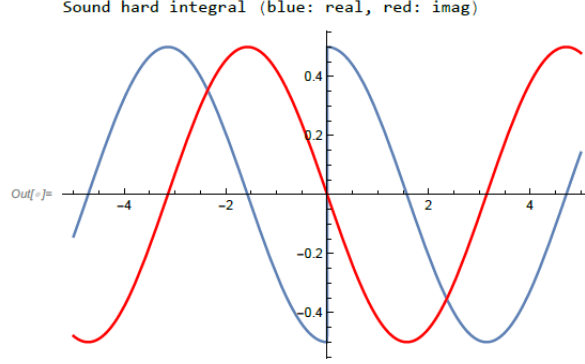


Figure: The surface S lies along y -axis and the plotted lines are the sound-hard integration result

In order to deal with this discontinuity, the principal value of the integral in equation (2.9) can be determined analytically as follows.

Let S be a flat plate of infinite extent in the X - Y plane with $\hat{n} = \hat{z}$ and $\sigma(\mathbf{r}') = 1$ everywhere on the plate. The observation point is located at $\mathbf{r} = (\rho = 0, \phi = 0, z)$, $z > 0$. The scalar Green's function can be expressed as

$$G(\mathbf{r}, \mathbf{r}') = \frac{e^{-jk|\mathbf{r}-\mathbf{r}'|}}{4\pi|\mathbf{r}-\mathbf{r}'|} = \frac{e^{-jk\sqrt{\rho'^2 + (z-z')^2}}}{4\pi\sqrt{\rho'^2 + (z-z')^2}}$$

The integral in equation (2.9) becomes

$$\oint_S \frac{\partial G(\mathbf{r}, \mathbf{r}')}{\partial n'} \sigma(\mathbf{r}') dS' = \int_0^\infty \int_0^{2\pi} \left[\frac{ze^{-jk|\mathbf{r}-\mathbf{r}'|}}{4\pi|\mathbf{r}-\mathbf{r}'|^3} + \frac{jkze^{-jk|\mathbf{r}-\mathbf{r}'|}}{4\pi|\mathbf{r}-\mathbf{r}'|^2} \right] \rho' d\phi' d\rho' = \frac{e^{-jkz}}{2} \text{ if } \text{Re}\{z\} \neq 0 \text{ and } \text{Im}\{k\} \leq 0$$

Letting $z \rightarrow 0$ yields the principal value of the integral

$$\lim_{z \rightarrow 0} \frac{e^{-jkz}}{2} = \frac{1}{2}$$

Of course, this is derived using a simple geometry and $\sigma(\mathbf{r}') = 1$. To understand what the principal value is for a general problem see figure 3 below. First, recall that $\frac{\partial G}{\partial n} = \nabla G \cdot \hat{n}$. The sub-figure 1 depicts the contributions of sources far from the observation point when propagated by the gradient of the scalar Green's function. There is a significant contribution from both sources because $\frac{\partial G}{\partial n}$ is appreciable. In sub-figure 2, when the observation point is infinitesimally close to the surface containing the sources, $\frac{\partial G}{\partial n} \rightarrow 0$ due to sources far away because ∇G is nearly tangential to the surface. Looking at sub-figure 3, when the observation point is still infinitesimally close to the surface, but highlighting contributions from nearby sources, there is a significant contribution—far more noticeable than from sources shown in sub-figure 2. One can now conclude that only the self-interactions will contribute to the integral when $\mathbf{r} \rightarrow \mathbf{r}'$. Additionally, the value of $\sigma(\mathbf{r}')$ can be

arbitrary since only the local effect matters. This holds true for all locally flat surfaces, but not for curved surfaces.

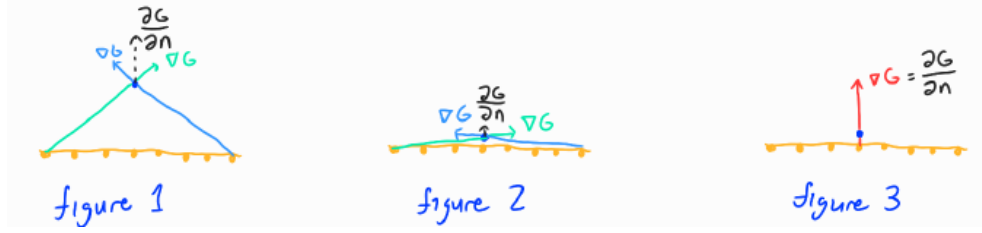


Figure 3: Local interactions dominate the integral when observing near the sources

The one-half from above becomes

$$\lim_{\mathbf{r} \rightarrow \mathbf{r}'} \iint_S \frac{\partial G(\mathbf{r}, \mathbf{r}')}{\partial n'_1} \sigma(\mathbf{r}') dS' = \frac{\sigma(\mathbf{r})}{2} \quad (3.4)$$

Thus equation (3.4) becomes computationally friendly expressed as

$$-\phi^{inc}(\mathbf{r}) = -\frac{\sigma(\mathbf{r})}{2} + \text{p.v.} \iint_S \frac{\partial G(\mathbf{r}, \mathbf{r}')}{\partial n'_1} \sigma(\mathbf{r}') dS' \quad (3.5)$$

Where the principal value integration excludes when $\mathbf{r}' = \mathbf{r}$.

3.3.3 Sound-Soft Combined Field Integral Equation (CFIE)

The sound-soft and sound-hard integral equations derived in the previous section suffer from resonance issues that make them poor choices when solving problems at mid- to high-frequencies. Looking at equation (3.2), if there was a scenario in which the LHS, $-\phi^{inc}(\mathbf{r})$, was zero on S , then the sources, $\sigma(\mathbf{r}')$, would mathematically not have a unique solution while a unique solution to this problem physically does exist. The same can occur for the sound-soft normal derivative IE. This is the pitfall of the integral equation formulation in that it does not guarantee a unique solution.

Consider a spherical scatterer with an incident spherical wave as an example. The theoretical scenario above occurs at the complimentary problem's resonant frequencies. These will sometimes be referred to as mathematical resonances of the sound-soft integral equation. In other words, at the frequencies/modes when a standing wave exists inside a spherical cavity, the field on the surface of the cavity are zero and solving the sound-soft IE for this problem will not produce the correct surface sources. These modes only exist when the cavity becomes comparable in size to the wavelength and become more and more common the higher the frequency (or lower the wavelength) becomes hence the sound-soft IE only works predictably well for low frequency problems. Though there is no simple physical example, the sound-hard IE will suffer from the same problem.

Realistic geometries will not be perfect spherical scatterers with perfect incident spherical waves; however, this problem still exists. Any closed scatterer is subject to mathematical resonances that hold no physical meaning, but cause there to be no unique solution to the integral equation.

To avoid the resonances, consider the general sound-soft IE, equation (3.1), once more

$$\phi^{sca}(\mathbf{r}) = \mathcal{L}[\sigma(\mathbf{r}')] = \iint_S G(\mathbf{r}, \mathbf{r}') \sigma(\mathbf{r}') dS' \quad (3.6)$$

Where $\sigma(\mathbf{r}') = -\frac{\partial\phi(\mathbf{r}')}{\partial n_1}$. As done for the sound-soft normal derivative IE, take the derivative with respect to the unprimed \hat{n}_1 direction of the surface of the scatterer.

$$\frac{\partial\phi^{sca}(\mathbf{r})}{\partial n_1} = \frac{\partial}{\partial n_1} \mathcal{L}[\sigma(\mathbf{r}')] = \iint_S \frac{\partial G(\mathbf{r}, \mathbf{r}')}{\partial n_1} \sigma(\mathbf{r}') dS' \quad (3.7)$$

Recalling that $\phi(\mathbf{r}) = \phi^{inc}(\mathbf{r}) + \phi^{sca}(\mathbf{r})$ and taking the normal derivative

$$\begin{aligned} \frac{\partial\phi(\mathbf{r})}{\partial n_1} &= \frac{\partial\phi^{inc}(\mathbf{r})}{\partial n_1} + \frac{\partial\phi^{sca}(\mathbf{r})}{\partial n_1} \\ \frac{\partial\phi^{sca}(\mathbf{r})}{\partial n_1} &= -\sigma(\mathbf{r}) - \frac{\partial\phi^{inc}(\mathbf{r})}{\partial n_1} \end{aligned}$$

Substituting this into equation (3.7)

$$-\sigma(\mathbf{r}) - \frac{\partial\phi^{inc}(\mathbf{r})}{\partial n_1} = \frac{\partial}{\partial n_1} \mathcal{L}[\sigma(\mathbf{r}')] = \iint_S \frac{\partial G(\mathbf{r}, \mathbf{r}')}{\partial n_1} \sigma(\mathbf{r}') dS' \quad (3.8)$$

The integral is discontinuous at $\mathbf{r} = \mathbf{r}'$ just as the sound-hard IE is and therefore the same principal value technique can be applied with a sign-change due to the derivative being with respect to unprimed variables yielding

$$\begin{aligned} -\sigma(\mathbf{r}) - \frac{\partial\phi^{inc}(\mathbf{r})}{\partial n_1} &= -\frac{\sigma(\mathbf{r})}{2} + \text{p.v.} \iint_S \frac{\partial G(\mathbf{r}, \mathbf{r}')}{\partial n_1} \sigma(\mathbf{r}') dS' \\ -\frac{\partial\phi^{inc}(\mathbf{r})}{\partial n_1} &= \frac{\sigma(\mathbf{r})}{2} + \text{p.v.} \iint_S \frac{\partial G(\mathbf{r}, \mathbf{r}')}{\partial n_1} \sigma(\mathbf{r}') dS' \end{aligned} \quad (3.9)$$

Let $\alpha \in [0,1]$ be an arbitrary weighing constant and we scale equation (3.9) by j to make the CFIE non-resonant (see proof below), Multiply equation (3.9) by $j(1-\alpha)$, equation (3.6) by α and sum them to form the sound-soft CFIE restricting $\mathbf{r} \in S$ so that $\phi^{sca}(\mathbf{r}) = -\phi^{inc}(\mathbf{r})$.

$$\begin{aligned} -\alpha\phi^{inc}(\mathbf{r}) - j(1-\alpha)\frac{\partial\phi^{inc}(\mathbf{r})}{\partial n_1} &= \alpha\mathcal{L}[\sigma(\mathbf{r}')] + j(1-\alpha)\frac{\partial}{\partial n_1} \mathcal{L}[\sigma(\mathbf{r}')] \quad \forall \mathbf{r} \in S \\ &= \alpha \iint_S G(\mathbf{r}, \mathbf{r}') \sigma(\mathbf{r}') dS' + j(1-\alpha) \frac{\sigma(\mathbf{r})}{2} \\ &\quad + j(1-\alpha) \text{p.v.} \iint_S \frac{\partial G(\mathbf{r}, \mathbf{r}')}{\partial n_1} \sigma(\mathbf{r}') dS' \quad \forall \mathbf{r} \in S \end{aligned} \quad (3.10)$$

Non-Resonance Proof

Consider the sound-soft CFIE without the weights α and with the normal derivative terms scaled by an unknown constant β

$$-\phi^{inc}(\mathbf{r}) - \beta \frac{\partial\phi^{inc}(\mathbf{r})}{\partial n_1} = \mathcal{L}[\sigma(\mathbf{r}')] + \beta \frac{\partial}{\partial n_1} \mathcal{L}[\sigma(\mathbf{r}')] \quad \forall \mathbf{r} \in S \quad (3.11)$$

To ensure that the CFIE does not suffer from the same resonance issues as the sound-soft and sound-hard IEs, there must be a condition on β . In order for the CFIE to be non-resonant

$$-\phi^{inc}(\mathbf{r}) - \beta \frac{\partial \phi^{inc}(\mathbf{r})}{\partial n_1} = 0 \text{ only when } \sigma(\mathbf{r}') = 0 \text{ on } S \quad (3.12)$$

Let $v = \mathcal{L}[\sigma(\mathbf{r}')] = -\phi^{inc}(\mathbf{r})$ and apply Green's theorem to v and its complex conjugate v^* on S and V_{int} where S is the surface sitting an infinitesimal distance within the scatterer surface and V_{int} is the volume circumscribed by it.

$$\iiint_{V_{int}} v \nabla^2 v^* - v^* \nabla^2 v \, dV = \iint_S v \frac{\partial v^*}{\partial n_1} - v^* \frac{\partial v}{\partial n_1} \, dS \quad (3.13)$$

When restricting $\mathbf{r} \in S$ we can also say that $v = \mathcal{L}[\sigma(\mathbf{r}')] = -\phi^{inc}(\mathbf{r}) = \phi^{sca}(\mathbf{r})$ due to the sound-soft boundary condition so in imposing the non-resonance in equation (3.17) it can also be stated that

$$v + \beta \frac{\partial v}{\partial n_1} = 0 \, \forall \, \mathbf{r} \in S \quad (3.14)$$

Returning to equation (3.13), since V_{int} does not include the boundary S where the sources lie, then v and v^* must obey the homogeneous wave equation inside V_{int} and the LHS of the above equation becomes 0.

$$0 = \iint_S v \frac{\partial v^*}{\partial n_1} - v^* \frac{\partial v}{\partial n_1} \, dS$$

Substituting in equation (3.14)

$$\begin{aligned} 0 &= \iint_S -\beta \frac{\partial v}{\partial n_1} \frac{\partial v^*}{\partial n_1} + \beta^* \frac{\partial v}{\partial n_1} \frac{\partial v^*}{\partial n_1} \, dS \\ &= -2j \text{Im}\{\beta\} \iint_S \left| \frac{\partial v}{\partial n_1} \right|^2 \, dS \end{aligned} \quad (3.15)$$

If β is restricted such that $\text{Im}\{\beta\} \neq 0$, then equation (3.15) will only be zero when $\left| \frac{\partial v}{\partial n_1} \right| = 0$ on S . It is well understood from discussions on the sound-hard IE in section 0 that when there are non-zero sources on S , then there will be a jump discontinuity across S in $\frac{\partial v}{\partial n_1}$ therefore the LHS will only be zero when $\sigma(\mathbf{r}') = 0$. This proves the sound-soft CFIE is non-resonant as long as $\text{Im}\{\beta\} \neq 0$. Going forward we set $\beta = j$.

3.3.4 Sound-Hard Combined Field Integral Equation (CFIE)

As with the sound-soft integral equation, the sound-hard integral equation suffers from resonances; however, these do not have an easily interpreted physical meaning. Using the sound-hard combined field integral equation eliminates this problem. Forming the sound-hard CFIE follows the same process as with the sound-soft CFIE. Starting with the sound-hard IE

$$\phi^{sca}(\mathbf{r}) = \iint_S \sigma(\mathbf{r}') \frac{\partial G(\mathbf{r}, \mathbf{r}')}{\partial n'_1} \, dS' \quad (3.16)$$

Take the normal derivative with respect to $\hat{\mathbf{n}}_1$ direction

$$\frac{\partial \phi^{sca}(\mathbf{r})}{\partial n_1} = \iint_S \sigma(\mathbf{r}') \frac{\partial^2 G(\mathbf{r}, \mathbf{r}')}{\partial n_1 \partial n'_1} \, dS'$$

Due to the boundary condition on S $\frac{\partial \phi^{sca}(\mathbf{r})}{\partial n_1} = -\frac{\partial \phi^{inc}(\mathbf{r})}{\partial n_1}$ and

$$-\frac{\partial \phi^{inc}(\mathbf{r})}{\partial n_1} = \iint_S \sigma(\mathbf{r}') \frac{\partial^2 G(\mathbf{r}, \mathbf{r}')}{\partial n_1 \partial n'_1} dS' \quad (3.17)$$

Let $\alpha \in [0,1]$ be an arbitrary weighing constant. Multiply equation (3.5) by α , multiply equation (3.17) by $(1 - \alpha)$ and sum them to form the sound-hard IE

$$\begin{aligned} -\alpha \phi^{inc}(\mathbf{r}) - (1 - \alpha) \frac{\partial \phi^{inc}(\mathbf{r})}{\partial n_1} \\ = -\alpha \frac{\sigma(r)}{2} + \alpha \text{p.v.} \iint_S \frac{\partial G(\mathbf{r}, \mathbf{r}')}{\partial n'_1} \sigma(\mathbf{r}') dS' + (1 - \alpha) \iint_S \sigma(\mathbf{r}') \frac{\partial^2 G(\mathbf{r}, \mathbf{r}')}{\partial n_1 \partial n'_1} dS' \end{aligned} \quad (3.18)$$

Special treatment of the last integral in equation (3.18) is required and to be determined later.

4 METHOD OF MOMENTS

The process of discretizing the integral equations can be done using the Method of Moments (MoM). The geometry of the scatterer is first discretized into N elements. In this case, (as is the case in my code) planar triangle elements will be used to form the so-called mesh for the scatterer. The method of moments discretization process will be first demonstrated starting with the sound-soft integral equation

4.1 SOUND-SOFT

Step one is discretizing the sources on the mesh using a set of basis functions. While any sufficient basis may be used, linear pulse functions will be used here defined as

$$\Pi_n(\mathbf{r}) = \begin{cases} 1, & \forall \mathbf{r} \text{ on element } n \\ 0, & \text{otherwise} \end{cases} \quad (4.1)$$

Therefore, the sources $\sigma(\mathbf{r}')$ can be approximately represented on the mesh as

$$\sigma(\mathbf{r}') \cong \sum_{n=1}^N \sigma_n \Pi_n(\mathbf{r}') \quad (4.2)$$

Where σ_n is the weight of the associated basis function.

$$\begin{aligned} -\phi^{inc}(\mathbf{r}) &= \iint_S G(\mathbf{r}, \mathbf{r}') \sigma(\mathbf{r}') dS' \\ &\cong \iint_S G(\mathbf{r}, \mathbf{r}') \sum_{n=1}^N \sigma_n \Pi_n(\mathbf{r}') dS' \\ &= \sum_{n=1}^N \sigma_n \iint_{S_n} G(\mathbf{r}, \mathbf{r}') \Pi_n(\mathbf{r}') dS' \end{aligned} \quad (4.3)$$

Where the integral is now over the surface of the n -th element only. The next step is known as the testing procedure which will provide a matrix equation with which the weights, σ_n , can be solved for. The left and right sides of equation (4.3) are multiplied by the so-called testing basis functions which for convenience will be the pulse basis functions defined in equation (4.2), but do not need to match the source basis functions. Following this, both sides are integrated over the test element.

$$-\iint_{S_m} \phi^{inc}(\mathbf{r}) \Pi_m(\mathbf{r}) dS = \sum_{n=1}^N \sigma_n \iint_{S_m} \iint_{S_n} G(\mathbf{r}, \mathbf{r}') \Pi_n(\mathbf{r}') \Pi_m(\mathbf{r}) dS' dS \quad (4.4)$$

When considering all $m \in [1, N]$ this forms a matrix equation

$$\begin{aligned} \mathbf{ZJ} &= \mathbf{V} \\ \mathbf{z}_{mn} &= \iint_{S_m} \iint_{S_n} G(\mathbf{r}, \mathbf{r}') \Pi_n(\mathbf{r}') \Pi_m(\mathbf{r}) dS' dS \\ \mathbf{v}_m &= -\iint_{S_m} \phi^{inc}(\mathbf{r}) \Pi_m(\mathbf{r}) dS \\ \mathbf{j}_n &= \sigma_n \end{aligned} \quad (4.5)$$

Where \mathbf{Z} is a square matrix of size $N \times N$ and \mathbf{J} and \mathbf{V} are column vectors of size N .

Need to add MoM implementation of soft normal derivative IE

4.2 SOUND-SOFT CFIE

We can now use MoM terminology and notation to glean more insight in to the mathematical resonance problem of the non-combined field integral equations. At or near these resonances, the excitation vector, \mathbf{V} , becomes closer and closer to zero and the condition number of the matrix \mathbf{Z} spikes. These become more frequent the higher the frequency is. At these spikes, it is unlikely any solver will converge to the true solution to the problem. To alleviate this problem, we want an integral equation formulation in which \mathbf{V} is only zero when the surface sources themselves are zero. To achieve this, we introduce the combined field integral equation (CFIE) which can be formed with either sound-soft or sound-hard boundary conditions.

The sound-soft CFIE is discretized following the same procedure as for the sound-soft IE. First substitute in the discretized form of the source terms given by equation (4.2) into equation (3.10)

$$\begin{aligned} & -\alpha \phi^{inc}(\mathbf{r}) - j(1 - \alpha) \frac{\partial \phi^{inc}(\mathbf{r})}{\partial n_1} \\ & = \alpha \sum_{n=1}^N \sigma_n \iint_S G(\mathbf{r}, \mathbf{r}') \Pi_n(\mathbf{r}') dS' + j(1 - \alpha) \sum_{n=1}^N \frac{\sigma_n}{2} \Pi_n(\mathbf{r}) \\ & \quad + j(1 - \alpha) \sum_{n=1}^N \sigma_n \text{p.v.} \iint_S \frac{\partial G(\mathbf{r}, \mathbf{r}')}{\partial n_1} \Pi_n(\mathbf{r}') dS' \end{aligned} \quad (4.6)$$

The testing procedure is then applied

$$\begin{aligned} & -\alpha \iint_{S_m} \phi^{inc}(\mathbf{r}) \Pi_m(\mathbf{r}) dS - j(1 - \alpha) \iint_{S_m} \frac{\partial \phi^{inc}(\mathbf{r})}{\partial n_1} \Pi_m(\mathbf{r}) dS \\ & = \alpha \sum_{n=1}^N \sigma_n \iint_{S_m} \iint_{S_n} G(\mathbf{r}, \mathbf{r}') \Pi_n(\mathbf{r}') \Pi_m(\mathbf{r}) dS' dS \\ & \quad + j(1 - \alpha) \sum_{n=1}^N \frac{\sigma_n}{2} \iint_{S_m} \Pi_n(\mathbf{r}) \Pi_m(\mathbf{r}) dS \\ & \quad + j(1 - \alpha) \sum_{n=1}^N \sigma_n \iint_{S_m} \text{p.v.} \iint_{S_n} \frac{\partial G(\mathbf{r}, \mathbf{r}')}{\partial n_1} \Pi_n(\mathbf{r}') \Pi_m(\mathbf{r}) dS' dS \end{aligned} \quad (4.7)$$

Noting that

$$\begin{aligned} & -\alpha \iint_{S_m} \phi^{inc}(\mathbf{r}) \Pi_m(\mathbf{r}) dS - j(1 - \alpha) \iint_{S_m} \frac{\partial \phi^{inc}(\mathbf{r})}{\partial n_1} \Pi_m(\mathbf{r}) dS \\ & = \sum_{n=1}^N \sigma_n \left[\alpha \iint_{S_m} \iint_{S_n} G(\mathbf{r}, \mathbf{r}') \Pi_n(\mathbf{r}') \Pi_m(\mathbf{r}) dS' dS \right. \\ & \quad \left. + j(1 - \alpha) \left(\frac{1}{2} \iint_{S_m} \Pi_n(\mathbf{r}) \Pi_m(\mathbf{r}) dS + \iint_{S_m} \text{p.v.} \iint_{S_n} \frac{\partial G(\mathbf{r}, \mathbf{r}')}{\partial n_1} \Pi_n(\mathbf{r}') \Pi_m(\mathbf{r}) dS' dS \right) \right] \end{aligned} \quad (4.8)$$

Which is a matrix equation where

$$\mathbf{z}_{mn} = \iint_{S_m} \iint_{S_n} G(\mathbf{r}, \mathbf{r}') \Pi_n(\mathbf{r}') \Pi_m(\mathbf{r}) dS' dS$$

$$\begin{aligned}
\mathbf{Z}_{mn}^{ND} &= \frac{1}{2} \iint_{S_m} \Pi_n(\mathbf{r}) \Pi_m(\mathbf{r}) dS + \iint_{S_m} \text{p.v.} \iint_{S_n} \frac{\partial G(\mathbf{r}, \mathbf{r}')}{\partial n_1} \Pi_n(\mathbf{r}') \Pi_m(\mathbf{r}) dS' dS \\
\mathbf{V}_m &= - \iint_{S_m} \phi^{inc}(\mathbf{r}) \Pi_m(\mathbf{r}) dS \\
\mathbf{V}_m^{ND} &= - \iint_{S_m} \frac{\partial \phi^{inc}(\mathbf{r})}{\partial n_1} \Pi_m(\mathbf{r}) dS \\
\mathbf{J}_n &= \sigma_n
\end{aligned} \tag{4.9}$$

Then equation (4.8) more succinctly becomes

$$\alpha \mathbf{V} + j(1 - \alpha) \gamma \mathbf{V}^{ND} = \mathbf{J}(\alpha \mathbf{Z} + j(1 - \alpha) \gamma \mathbf{Z}^{ND}) \tag{4.10}$$

Note that in practice, the first term in \mathbf{Z}_{mn}^{ND} is simply implemented in code when the spatial basis functions are pulse functions. The integrand is only nonzero when $n = m$ then

$$\frac{1}{2} \iint_{S_m} \Pi_n(\mathbf{r}) \Pi_m(\mathbf{r}) dS = \frac{\delta_{nm} A_m}{2}$$

Where δ_{nm} is the Kronecker delta and A_m is the area of element m .

~~In my code, an additional scale factor of γ is added to the \mathbf{V}^{ND} and \mathbf{Z}^{ND} terms to normalize the magnitudes of the vector/matrix entries to those in \mathbf{V} and \mathbf{Z} .~~

$$\gamma = \frac{\sum_{ij} |\mathbf{Z}_{ij}|}{\sum_{ij} |\mathbf{Z}_{ij}^{ND}|}$$

4.3 NUMERICAL INTEGRATION

Computing the continuous integrals in equations (4.3) requires numerical integration (a.k.a. quadrature) routines to be done efficiently. The routine employed in my integral equation code is Gaussian quadrature

4.3.1 Gaussian Quadrature

Gaussian quadrature approximates integration over any smooth function that can be well represented by a set of polynomial functions. An N -point Gaussian quadrature rule will exactly integrate a polynomial of degree $2N - 1$. These work well for the integrands encountered in acoustic scattering as they are smooth functions with sinusoidal variations in the far- and near-field regions. There are discontinuities that arise for self-interactions that require special handling which will be discussed later. The following is the Gaussian quadrature function

$$\int_{-1}^1 f(x) dx \approx \sum_{i=1}^n w_i f(x_i) \tag{4.11}$$

That is, the integral over $f(x)$ from $[-1, 1]$ is approximately equal to the sum of $f(x)$ evaluated at the quadrature points x_i and weighted by the corresponding quadrature weights w_i . The set of quadrature points and weights can be chosen to best suit the application. In general, choosing more points will result in more accurate integration.

For the case of integration over triangles, there are well-defined rules to choose from in literature. For triangles with a surface denoted by S in my code, equation (4.11) becomes

$$\iint_S f(\mathbf{r}) dS \approx A \sum_{i=1}^n w_i f(\mathbf{r}_i) \quad (4.12)$$

Where A is the area of the triangle. Scaling by the area is done because the quadrature rules are defined such that $\sum_{i=1}^n w_i = 1$ i.e. the rule is designed to integrate a triangle with unit area so for a general triangle we must scale by its area.

The actual quadrature rules used in my code are given here:

https://www.math.unipd.it/~alvise/SETS_CUBATURE_TRIANGLE/dunavant/set_dunavant_barycentric.m

Rules for integrating triangles are generally defined in terms of barycentric coordinates to generalize them for any triangle.

Barycentric Coordinates

Also known as simplex or area coordinates, barycentric coordinates on triangles are a local coordinate system. They are defined such that

$$\mathbf{r} = \mathbf{v}_1 \xi_1 + \mathbf{v}_2 \xi_2 + \mathbf{v}_3 \xi_3$$

Where \mathbf{r} is a location in cartesian coordinates corresponding to the location in barycentric coordinates given by (ξ_1, ξ_2, ξ_3) and \mathbf{v}_i is the cartesian coordinates of the i -th triangle vertex. As one can see, a location in barycentric coordinates is relative to the triangle it is defined with respect to and therefore allows for representation of quadrature points that work for any shaped triangle.

The name “area” coordinates is perhaps the most insightful because each component ξ_i of a coordinate is a normalized area of a sub-triangle formed by the vertices \mathbf{r} , \mathbf{v}_{i-1} and \mathbf{v}_{i+1} . As such, all three components are not independent and knowledge of two out of three is enough to determine the location with the following relation

$$\xi_i = 1 - \xi_{i-1} - \xi_{i+1}$$

Add cartesian to barycentric

Applying equation (4.12) to equations (4.5) gives a fully discretized expression for the matrix and right hand side (RHS) entries such that the unknowns σ_n can be solved for

$$\begin{aligned} \mathbf{z}_{mn} &= A_m A_n \sum_{i=1}^p \left[w_i \Pi_m(\mathbf{r}_i) \sum_{j=1}^q w_j G(\mathbf{r}_i, \mathbf{r}_j) \Pi_n(\mathbf{r}_j) \right] \\ \mathbf{v}_m &= -A_m \sum_{i=1}^p w_i \phi^{inc}(\mathbf{r}_i) \Pi_m(\mathbf{r}_i) \\ \mathbf{J}_n &= \sigma_n \end{aligned} \quad (4.13)$$

Note that the test and source quadrature rules do not need to be equivalent.

4.4 INTEGRATION ROUTINES

There are different ways integration must be handled depending on where the test and source elements are located with respect to one another. For well separated elements, equations (4.13) as-is will provide accurate results. When the elements are close to one another the Green's function becomes singular due to $G(\mathbf{r}, \mathbf{r}') \propto \frac{1}{|\mathbf{r}-\mathbf{r}'|}$ and integration must be handled differently. There are two singular cases: 1) two different elements near each other interacting and 2) an element interacting with itself.

Far-Field Integration

As stated above, this is done by directly computing equations (4.13).

Near-Field Integration

This is singular case 1 from above. Element pairs falling into this category are determined by an input parameter to the solve functions that dictate a maximum distance between element centroids that when exceeded constitute a far-field interaction and when within the distance are near-field except for the case when the test and source elements are the same. Integration for the \mathbf{Z} matrix entries of near-field pairs uses singularity subtraction from the Green's function followed by numerical integration of the non-singular term and analytical integration of the singular term as shown below.

$$\begin{aligned} G(r, r') &= \frac{e^{-jkR}}{4\pi R} - \frac{1}{4\pi R} + \frac{1}{4\pi R} \\ &= \frac{e^{-jkR} - 1}{4\pi R} + \frac{1}{4\pi R} \\ &= \tilde{G}(R) + S(R) \end{aligned} \tag{4.14}$$

The left term is integrated numerically and the right term has a purely analytical integration routine as defined in "Potential Integrals for Uniform and Linear Source Distributions on Polygonal and Polyhedral Domains" by Wilton et al. in the section titled *Surface Sources Distributed on Polygons*.

Self-Interactions

The third case for integration is when the test and source elements are one in the same. As for the near-field interactions, the singularity is subtracted like in equation (4.14) and the right term is handled with the same analytical routine. The left term, however, is handled differently. Even though the term is not singular, it is discontinuous as shown in the plot below

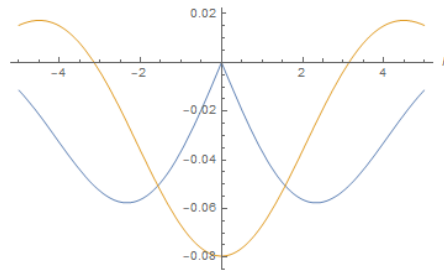


Figure 1: Plot of real (blue) and imaginary (orange) components of $\tilde{G}(R)$ (y-axis) demonstrating its discontinuity at $R = 0$ (x-axis).

As discussed in the Gaussian quadrature section, this numerical integration rule only works for curves that can be well approximated by polynomials and discontinuities cannot. To avoid this issue, the triangle/element being integrated over is split into three sub-triangles as shown below.

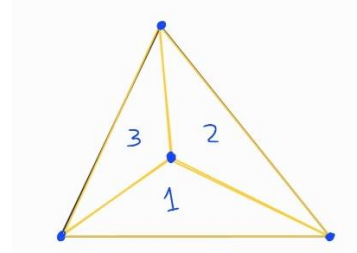


Figure 2: Triangle divided into three sub-triangles. Central node is the testing location dictated by the test quadrature rule used.

Because the discontinuity is located at the central node, from the perspective of each sub-triangle, the discontinuity is simply the end of the integration domain. Equation (4.5) (elements of \mathbf{Z} prior to discretization) effectively becomes

$$\mathbf{Z}_{mn} = \iint_{S_m} \Pi_m(\mathbf{r}) \left[\iint_{S_{n1}} G(\mathbf{r}, \mathbf{r}') \Pi_{n1}(\mathbf{r}') dS' + \iint_{S_{n2}} G(\mathbf{r}, \mathbf{r}') \Pi_{n2}(\mathbf{r}') dS' + \iint_{S_{n3}} G(\mathbf{r}, \mathbf{r}') \Pi_{n3}(\mathbf{r}') dS' \right] dS \quad (4.15)$$

Where the three source integrals are each over one of the sub-triangles. Gaussian quadrature is applied to each integral as before, but it is not written out for succinctness.

5 SCATTERING MATRIX

The scattering matrix provides a means of computing the outgoing fields on $d\Omega_f$, a fictitious spherical surface surrounding the scatterer in its far field, from the incoming fields. To provide physical intuition, imagine a spherical scatterer with an incident spherical wave of degree ℓ and order m . The only wave reflected from the scatterer will be a spherical wave of degree ℓ and order m because it is a perfect sphere and a scattering “matrix” of size 1×1 can be formed by the scattering coefficient Γ . If the incident wave contains N harmonics of spherical waves, then the scattering matrix becomes a diagonal matrix of size $N \times N$ where the diagonal elements correspond to the reflection coefficients for each harmonic. If the geometry is changed to an arbitrary non-spherical shape, then the scattering matrix will lose its diagonal property because the non-spherical geometric features cause coupling between incident and reflected waves of different harmonics.

Mathematically, the scattering matrix is a unitless matrix, \mathbf{S} , that relates a set of incoming waves to a set of outgoing waves in the far-field

$$\mathcal{O}_{t,||}(r) = S_{tp} \mathcal{J}_{p,||}^*(r)$$

Where $\mathcal{O}_{t,||}(kr)$ is the outgoing wave of t -th mode (or harmonic) on $d\Omega_f$, $\mathcal{J}_{p,||}^*(kr)$ is the complex conjugate of the incoming wave of p -th mode on $d\Omega_f$ and S_{tp} is the entry of \mathbf{S} in the t -th row and p -th column. Each entry of \mathbf{S} relates a specific incoming mode from a defined set of modes to another mode in the same set.

In theory, a scattering matrix relates any arbitrary set of incoming modes to outgoing modes. However, to completely define the scattering properties of an object, all possible modes would be required. In practice, as higher and higher modes are sent in, the electrical size of the object decreases and the matrix can be truncated as the scattering coefficients will go to zero. There is more on this later in the section.

5.1.1 Acoustic Derivation

The acoustic scattering matrix is first derived from the sound-soft integral equation.

$$\begin{aligned} \phi_{p,||}^{\text{sca}}(\mathbf{r}) &= \mathcal{L}_{||} \left[\sigma_p^s(\mathbf{r}) \right] \\ &= \oint_S G_{\infty}(\mathbf{r}, \mathbf{r}') \sigma_p^s(\mathbf{r}') ds' \\ G_{\infty}(\mathbf{r}, \mathbf{r}') &= \frac{e^{-jkr}}{4\pi r} e^{jk\hat{\mathbf{r}} \cdot \mathbf{r}'} \end{aligned}$$

The first exponential term in the Green’s function can be rewritten using the asymptotic form of a Hankel function of the second kind and the second exponential term can be expanded in terms of spherical harmonics

$$\begin{aligned} h_{\ell,||}^{(2)}(kr) &= \lim_{r \rightarrow \infty} h_{\ell}^{(2)}(kr) = (j)^{\ell+1} \frac{e^{-jkr}}{kr} \Rightarrow \frac{e^{-jkr}}{r} = k(j)^{-(\ell+1)} h_{\ell,||}^{(2)}(kr) \\ e^{jk\hat{\mathbf{r}} \cdot \mathbf{r}'} &= \sum_{\ell=0}^{\infty} \sum_{m=-\ell}^{\ell} 4\pi (j)^{\ell} Y_{\ell m}^*(\theta, \phi) Y_{\ell m}(\theta', \phi') j_{\ell}(kr') \end{aligned}$$

Now we can write an expanded form of the Green's function

$$G_{\infty}(\mathbf{r}, \mathbf{r}') = \frac{k}{4\pi} (j)^{-(\ell+1)} h_{\ell,||}^{(2)}(kr) \sum_{\ell=0}^{\infty} \sum_{m=-\ell}^{\ell} 4\pi (j)^{\ell} Y_{\ell m}^*(\theta, \phi) Y_{\ell m}(\theta', \phi') j_{\ell}(kr')$$

Since ℓ is arbitrary, the terms outside the summation with ℓ -dependence can be distributed onto the terms within.

$$G_{\infty}(\mathbf{r}, \mathbf{r}') = -jk \sum_{\ell=0}^{\infty} \sum_{m=-\ell}^{\ell} h_{\ell,||}^{(2)}(kr) Y_{\ell m}^*(\theta, \phi) j_{\ell}(kr') Y_{\ell m}(\theta', \phi')$$

Finally, the scattered far-field can be written in an expanded form as

$$\phi_{p,||}^{\text{sca}}(\mathbf{r}) = -jk \oint_S \sum_{\ell=0}^{\infty} \sum_{m=-\ell}^{\ell} h_{\ell,||}^{(2)}(kr) Y_{\ell m}^*(\theta, \phi) j_{\ell}(kr') Y_{\ell m}(\theta', \phi') \sigma_p^s(\mathbf{r}') ds' \quad (2.10)$$

The scattered far-field is also defined to be

$$\begin{aligned} \phi_{p,||}^{\text{sca}}(\mathbf{r}) &= \sum_{t=1}^M \mathbf{P}_{tp} \mathcal{I}_{t,||}^*(kr) \\ \mathbf{P}_{tp} &= \frac{-j}{2k} \oint_S \phi_t^{\text{inc}}(\mathbf{r}') \sigma_p^s(\mathbf{r}') ds' \end{aligned} \quad (2.11)$$

Where $t = (\ell, m)^{\text{th}}$ term and can be expanded into two summations over ℓ and m as seen in the Green's function expansion above. Expanding the sum and substituting in \mathbf{P}_{tp} and equation (2.8) noting that $h_{\ell}^{(1)*}(kr) = h_{\ell}^{(2)}(kr)$ yields

$$\begin{aligned} \phi_t^{\text{inc}}(\mathbf{r}') &= 2kj_t(kr') Y_t(\theta', \phi') \\ \mathcal{I}_{t,||}^*(kr) &= kh_{t,||}^{(2)}(kr) Y_t^*(\theta, \phi) \\ \phi_{p,||}^{\text{sca}}(\mathbf{r}) &= \sum_{t=1}^M \frac{-j}{2k} \oint_S 2kj_t(kr') Y_t(\theta', \phi') \sigma_p^s(\mathbf{r}') ds' kh_{t,||}^{(2)}(kr) Y_t^*(\theta, \phi) \\ &= -jk \oint_S \sum_{\ell=0}^{\infty} \sum_{m=-\ell}^{\ell} h_{\ell,||}^{(2)}(kr) Y_{\ell m}^*(\theta, \phi) j_{\ell}(kr') Y_{\ell m}(\theta', \phi') \sigma_p^s(\mathbf{r}') ds' \end{aligned}$$

Which verifies that equation (2.11) is a valid expression for the scattered far-field.

The scattering matrix can now be defined as follows from previous expressions starting with total field.

$$\phi_{p,||}(\mathbf{r}) = \phi_{p,||}^{\text{inc}}(\mathbf{r}) + \phi_{p,||}^{\text{sca}}(\mathbf{r})$$

Expand the incident field using equation (2.8) and scattered fields using equation (2.11)

$$\phi_{p,||}(\mathbf{r}) = \mathcal{I}_p(kr) + \mathcal{O}_p(kr) + \sum_{t=1}^M \mathbf{P}_{tp} \mathcal{I}_{t,||}^*(kr)$$

The outgoing field and incoming field can be related as follows:

$$\begin{aligned}\mathcal{I}_{p,\parallel}(kr) &= kh_{\ell,\parallel}^{(1)}(kr)Y_{\ell m}(\theta, \phi) \\ \mathcal{I}_{p,\parallel}^*(kr) &= kh_{\ell,\parallel}^{(2)}(kr)Y_{\ell m}^*(\theta, \phi)\end{aligned}$$

Instead of the $p = (\ell, m)^{\text{th}}$ incoming field, let the incoming field be the $p = (\ell, -m)^{\text{th}}$ incoming field and applying the relation $Y_{\ell, -m}^*(\theta, \phi) = (-1)^m Y_{\ell m}(\theta, \phi)$

$$\begin{aligned}\mathcal{I}_{p,\parallel}^*(kr) &= (-1)^m kh_{\ell,\parallel}^{(2)}(kr)Y_{\ell m}(\theta, \phi) \\ &= (-1)^m \mathcal{O}_{p,\parallel}(kr)\end{aligned}$$

Substituting this back into the expression for $\phi_{p,\parallel}(\mathbf{r})$

$$\begin{aligned}\phi_{p,\parallel}(\mathbf{r}) &= \mathcal{I}_p(kr) + \mathcal{O}_p(kr) + \sum_{t=1}^M \mathbf{P}_{tp} \mathcal{I}_{t,\parallel}^*(kr) \\ &= \mathcal{I}_p(kr) + (-1)^m \mathcal{I}_{p,\parallel}^*(kr) + \sum_{t=1}^M \mathbf{P}_{tp} \mathcal{I}_{t,\parallel}^*(kr) \\ &= \mathcal{I}_p(kr) + \sum_{t=1}^M \left((-1)^m \delta_{pt} + \mathbf{P}_{tp} \right) \mathcal{I}_{t,\parallel}^*(kr) \\ &= \mathcal{I}_p(kr) + \sum_{t=1}^M \mathbf{S}_{tp} \mathcal{I}_{t,\parallel}^*(kr) \\ \mathbf{S}_{tp} &= (-1)^m \delta_{pt} + \mathbf{P}_{tp}\end{aligned}\tag{2.12}$$

Where \mathbf{S}_{tp} are entries of the scattering matrix, which relates the t^{th} incoming field to the total p^{th} outgoing field, and δ_{pt} is the Kronecker delta function.

Truncating the Scattering Matrix

The scattering matrix cannot contain all possible harmonics that excite the system or else it would be infinite in size. It turns out that the degree, ℓ , of the spherical harmonics can be truncated when $\ell \approx ka$ where k is the wavenumber and a is the largest dimension of the scatterer. This rule seems to only hold for electrically large objects and not when the size is less than or comparable to a wavelength.

5.1.2 Scattering Matrix Implementation

Fortunately, computation of the scattering matrix is straightforward with a Method of Moments code.

The scattering matrix formed by \mathbf{S}_{tp} can be separated into a sum of two matrices. The first matrix is the identity-like matrix formed by the entries

$$\mathbf{I}_{tp} = (-1)^m \delta_{pt}\tag{2.13}$$

The second matrix looks as follows

$$\begin{bmatrix} \mathbf{P}_{11} & \mathbf{P}_{12} & \cdots & \mathbf{P}_{1M} \\ \mathbf{P}_{21} & \mathbf{P}_{22} & \ddots & \vdots \\ \vdots & \ddots & \ddots & \vdots \\ \mathbf{P}_{M1} & \cdots & \cdots & \mathbf{P}_{MM} \end{bmatrix} \quad (2.14)$$

Upon further dissection

$$\frac{-j}{2k} \begin{bmatrix} \iint_S \phi_1^{\text{inc}}(\mathbf{r}') \sigma_1^s(\mathbf{r}') ds' & \cdots & \iint_S \phi_1^{\text{inc}}(\mathbf{r}') \sigma_M^s(\mathbf{r}') ds' \\ \vdots & \ddots & \vdots \\ \iint_S \phi_M^{\text{inc}}(\mathbf{r}') \sigma_1^s(\mathbf{r}') ds' & \cdots & \iint_S \phi_M^{\text{inc}}(\mathbf{r}') \sigma_M^s(\mathbf{r}') ds' \end{bmatrix}$$

Recall that in a MoM code, $\sigma_p^s(\mathbf{r})$ is represented as a sum of weighted basis functions

$$\sigma_p^s(\mathbf{r}) = \sum_{n=1}^N \sigma_{np}^s \Pi_n(\mathbf{r}) \quad (2.15)$$

The entries of the matrix above are discretized with the following representation

$$\iint_S \phi_t^{\text{inc}}(\mathbf{r}') \sigma_p^s(\mathbf{r}') ds' = \sum_{n=1}^N \sigma_{np}^s \iint_S \phi_t^{\text{inc}}(\mathbf{r}') \Pi_n(\mathbf{r}') ds'$$

And the matrix becomes

$$\frac{-j}{2k} \begin{bmatrix} \sum_{n=1}^N \sigma_{n1}^s \iint_S \phi_1^{\text{inc}}(\mathbf{r}') \Pi_n(\mathbf{r}') ds' & \cdots & \sum_{n=1}^N \sigma_{nM}^s \iint_S \phi_1^{\text{inc}}(\mathbf{r}') \Pi_n(\mathbf{r}') ds' \\ \vdots & \ddots & \vdots \\ \sum_{n=1}^N \sigma_{n1}^s \iint_S \phi_M^{\text{inc}}(\mathbf{r}') \Pi_n(\mathbf{r}') ds' & \cdots & \sum_{n=1}^N \sigma_{nM}^s \iint_S \phi_M^{\text{inc}}(\mathbf{r}') \Pi_n(\mathbf{r}') ds' \end{bmatrix}$$

Which can be written as the product of two matrices

$$\frac{j}{2k} \begin{bmatrix} -\iint_S \phi_1^{\text{inc}}(\mathbf{r}') \Pi_1(\mathbf{r}') ds' & \cdots & -\iint_S \phi_1^{\text{inc}}(\mathbf{r}') \Pi_N(\mathbf{r}') ds' \\ \vdots & \ddots & \vdots \\ -\iint_S \phi_M^{\text{inc}}(\mathbf{r}') \Pi_1(\mathbf{r}') ds' & \cdots & -\iint_S \phi_M^{\text{inc}}(\mathbf{r}') \Pi_N(\mathbf{r}') ds' \end{bmatrix} \begin{bmatrix} \sigma_{11}^s & \cdots & \sigma_{1M}^s \\ \vdots & \ddots & \vdots \\ \sigma_{N1}^s & \cdots & \sigma_{NM}^s \end{bmatrix} = \frac{j}{2k} \mathbf{V}_s^T \mathbf{J}_s \quad (2.16)$$

It is now clear that the left matrix's rows correspond to excitation vectors (or RHSs) of the sound-soft IE in a method of moments formulation for the p^{th} harmonic as denoted by \mathbf{V} in equation (4.5). The right matrix's columns correspond to source vectors (or solution vectors) in a method of moments formulation for the p^{th} harmonic as denoted by \mathbf{J} in equation (4.5). The final matrix equation for the scattering matrix can be written using (2.13) and (2.16) as

$$\mathbf{S} = \mathbf{I}_s + \frac{j}{2k} \mathbf{V}_s^T \mathbf{J}_s \quad (2.17)$$

The subscript s is to differentiate these matrices from the vectors in the method of moments formulations shown earlier.

5.1.2.1 Properties of the Scattering Matrix

The scattering matrix is unitary where \mathbf{I} is the identity matrix of equal dimension as \mathbf{S}

$$\mathbf{S}^\dagger \mathbf{S} = \mathbf{I} \quad (2.18)$$

The scattering matrix is symmetric

$$\mathbf{S} = \mathbf{S}^T \quad (2.19)$$

5.1.2.2 Frequency Derivative

The derivative of the scattering matrix with respect to frequency (i.e. wavenumber, k) is computed as follows

$$\mathbf{S}' = \frac{\partial \mathbf{S}}{\partial k} = \frac{\partial}{\partial k} \left[\mathbf{I}_s + \frac{j}{2k} \mathbf{V}_s^T \mathbf{J}_s \right] \quad (2.20)$$

Applying chain rule

$$\mathbf{S}' = \frac{-j}{2k^2} \mathbf{V}_s^T \mathbf{J}_s + \frac{j}{2k} \mathbf{V}_s'^T \mathbf{J}_s + \frac{j}{2k} \mathbf{V}_s^T \mathbf{J}_s' \quad (2.21)$$

Recalling that $\mathbf{ZJ} = \mathbf{V}$ in the method of moments

$$\begin{aligned} (\mathbf{ZJ}_s)' &= \mathbf{V}_s' \\ \mathbf{Z}'\mathbf{J}_s + \mathbf{Z}\mathbf{J}_s' &= \mathbf{V}_s' \\ \mathbf{J}_s' &= \mathbf{Z}^{-1} (\mathbf{V}_s' - \mathbf{Z}'\mathbf{J}_s) \end{aligned} \quad (2.22)$$

Additionally, it is true that for any system of equations where \mathbf{Z} is square

$$\mathbf{V}_s^T (\mathbf{Z}^{-1})^T = \mathbf{J}_s^T$$

Under full Galerkin testing (i.e. same basis and quadrature rules for test and source integrals), \mathbf{Z} becomes symmetric and

$$\mathbf{V}_s^T \mathbf{Z}^{-1} = \mathbf{J}_s^T \quad (2.23)$$

Substituting equations (2.22) and (2.23) into equation (2.21)

$$\begin{aligned}
\mathbf{S}' &= \frac{-j}{2k^2} \mathbf{V}_s^T \mathbf{J}_s + \frac{j}{2k} \mathbf{V}_s'^T \mathbf{J}_s + \frac{j}{2k} \mathbf{V}_s^T \mathbf{Z}^{-1} (\mathbf{V}_s' - \mathbf{Z}' \mathbf{J}_s) \\
&= \frac{-j}{2k^2} \mathbf{V}_s^T \mathbf{J}_s + \frac{j}{2k} \mathbf{V}_s'^T \mathbf{J}_s + \frac{j}{2k} \mathbf{J}_s^T \mathbf{V}_s' - \frac{j}{2k} \mathbf{J}_s^T \mathbf{Z}' \mathbf{J}_s
\end{aligned} \tag{2.24}$$

Now to compute the derivative of \mathbf{V}_s

$$\mathbf{V}_{np}' = -\iint_S \phi_p^{\text{inc}'}(\mathbf{r}') \Pi_n(\mathbf{r}') ds'$$

The incident field is given by equation (2.8) and its frequency derivative is

$$\begin{aligned}
\phi_p^{\text{inc}'}(\mathbf{r}) &= \frac{\partial}{\partial k} [2kj_\ell(kr)Y_{\ell m}(\theta, \phi)] \\
&= 2j_\ell(kr)Y_{\ell m}(\theta, \phi) + 2k \frac{\partial j_\ell(kr)}{\partial k} Y_{\ell m}(\theta, \phi) \\
&= 2j_\ell(kr)Y_{\ell m}(\theta, \phi) + 2kr \left(\frac{l}{kr} j_\ell(kr) - j_{\ell+1}(kr) \right) Y_{\ell m}(\theta, \phi) \\
&= 2Y_{\ell m}(\theta, \phi) ((\ell+1)j_\ell(kr) - krj_{\ell+1}(kr))
\end{aligned} \tag{2.25}$$

The frequency derivative of \mathbf{Z} is given by

$$\mathbf{Z}'_{mn} = \iint_S \iint_S \Pi_m(\mathbf{r}) G'(\mathbf{r}, \mathbf{r}') \Pi_n(\mathbf{r}') ds' ds \tag{2.26}$$

Where $G'(\mathbf{r}, \mathbf{r}') = \frac{-j}{4\pi} e^{-jk|\mathbf{r}-\mathbf{r}'|}$ which no longer has any singularities. \mathbf{Z}'_{mn} can be computed for non-

self-terms using standard Gaussian quadrature; however, due to the discontinuity at $|\mathbf{r}-\mathbf{r}'|=0$,

Gaussian quadrature is inaccurate since it is derived to approximate integrals well modeled by polynomials. The triangle splitting method in section 4.4 can be used for self-terms in the matrix since it effectively places the discontinuity on the boundary of the integrals.

6 WIGNER-SMITH EQUATION SECTION (NEXT)

6.1 INTRODUCTION

In acoustics, Wigner-Smith (WS) theory describes a methodology for characterizing acoustic scattering based on the dwell time of acoustic waves in a system using WS time-delay matrices given by

$$\mathbf{Q} = j\mathbf{S}^\dagger \mathbf{S}' \quad (6.1)$$

Where \mathbf{S} and \mathbf{S}' are the scattering matrix and its frequency derivative (with respect to k) given by equations (2.17) and (2.24). Diagonalizing \mathbf{Q} results in a set WS modes (eigenvectors) that describe a set of all possible incident fields (read: all incident fields included in construction of \mathbf{S}) that produce an outgoing wave with the corresponding dwell times (eigenvalues) in the system.

The diagonalization of \mathbf{Q} is as follows using equation (4.1) of the appendix

$$\mathbf{Q} = \mathbf{W} \bar{\mathbf{Q}} \mathbf{W}^\dagger \quad (3.1)$$

In which the columns of \mathbf{W} are the eigenvectors and $\bar{\mathbf{Q}}$ is a diagonal matrix of the eigenvalues.

6.2 DERIVATION OF \mathbf{Q}

6.2.1 One-port System

The figure below depicts an M -port network that is linear, time-invariant, lossless and reciprocal.

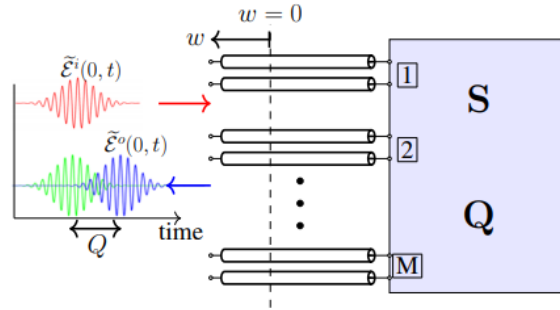


Figure: An M -port network characterized by \mathbf{S} and \mathbf{Q}

Let $M = 1$ and the incoming field on the line be

$$\phi^i(w, \omega) = e^{jk(\omega)w} \quad (3.2)$$

Where w is the distance away from the port towards the left in the figure and $k(\omega)$ is the propagation constant along the line. The outgoing field on the line is related to the incoming field by the scattering coefficient $S(\omega)$

$$\phi^o(w, \omega) = S(\omega) e^{-jk(\omega)w} = S(\omega) (\phi^i(w, \omega))^* \quad (3.3)$$

Since the network is lossless, the scattering coefficient has unity magnitude and can be written as

$$S(\omega) = e^{-j\gamma(\omega)} \quad (3.4)$$

Now let the incoming pulse be a narrowband signal, $\tilde{\phi}^i(w, t)$, with an envelope given by

$$\tilde{A}(t) = \int_{\omega_0 - \Delta\omega}^{\omega_0 + \Delta\omega} A(\omega - \omega_0) e^{j\omega t} d\omega$$

Centered at frequency ω_0 with a bandwidth of $2\Delta\omega$. The incoming signal is

$$\begin{aligned} \tilde{\phi}^i(w, t) &= \text{Re} \left\{ \int_{\omega_0 - \Delta\omega}^{\omega_0 + \Delta\omega} A(\omega - \omega_0) e^{j(\omega t + k(\omega)w)} d\omega \right\} \\ &= \text{Re} \left\{ \int_{\omega_0 - \Delta\omega}^{\omega_0 + \Delta\omega} A(\omega - \omega_0) e^{j(\omega t + (k(\omega_0) + k'(\omega_0)(\omega - \omega_0))w)} d\omega \right\} \\ &= \text{Re} \left\{ \int_{\omega_0 - \Delta\omega}^{\omega_0 + \Delta\omega} A(\omega - \omega_0) e^{j\omega(t + k'(\omega_0)w)} d\omega e^{jw(k(\omega_0) - \omega_0 k'(\omega_0))} \right\} \\ &= \text{Re} \left\{ \tilde{A}(t + k'(\omega_0)w) e^{j\omega_0(t + k'(\omega_0)w)} e^{jw(k(\omega_0) - \omega_0 k'(\omega_0))} \right\} \\ &= \text{Re} \left\{ \tilde{A}(t + k'(\omega_0)w) e^{j\omega_0 t} e^{jw(k(\omega_0))} \right\} \\ &= \tilde{A}(t + k'(\omega_0)w) \cos(\omega_0 t + k(\omega_0)w) \end{aligned} \quad (3.5)$$

In which $k(\omega) \cong k(\omega_0) + k'(\omega_0)(\omega - \omega_0) \forall \omega \in [\omega_0 - \Delta\omega, \omega_0 + \Delta\omega]$ due to the narrowband nature of the signal and the time-shifting and frequency-shifting properties were used to derive the final expression. The outgoing signal is determined via equation (3.3) to be

$$\begin{aligned} \tilde{\phi}^o(w, t) &= \text{Re} \left\{ \int_{\omega_0 - \Delta\omega}^{\omega_0 + \Delta\omega} S(\omega) A(\omega - \omega_0) e^{j(\omega t - k(\omega)w)} d\omega \right\} \\ &= \text{Re} \left\{ \int_{\omega_0 - \Delta\omega}^{\omega_0 + \Delta\omega} e^{-j\gamma(\omega)} A(\omega - \omega_0) e^{j(\omega t - k(\omega_0) - k'(\omega_0)(\omega - \omega_0)w)} d\omega \right\} \\ &= \text{Re} \left\{ \int_{\omega_0 - \Delta\omega}^{\omega_0 + \Delta\omega} A(\omega - \omega_0) e^{j\omega(t - wk'(\omega_0) - \gamma'(\omega_0))} e^{j(-wk(\omega_0) + wk'(\omega_0)\omega_0 - \gamma(\omega_0) + \gamma'(\omega_0)\omega_0)} d\omega \right\} \\ &= \text{Re} \left\{ \tilde{A}(t - k'(\omega_0)w - \gamma'(\omega_0)) e^{j\omega_0(t - wk'(\omega_0) - \gamma'(\omega_0))} e^{j(-wk(\omega_0) + wk'(\omega_0)\omega_0 - \gamma(\omega_0) + \gamma'(\omega_0)\omega_0)} \right\} \\ &= \text{Re} \left\{ \tilde{A}(t - k'(\omega_0)w - \gamma'(\omega_0)) e^{j(\omega_0 t - wk(\omega_0) - \gamma(\omega_0))} \right\} \\ &= \tilde{A}(t - k'(\omega_0)w - \gamma'(\omega_0)) \cos(\omega_0 t - k(\omega_0)w - \gamma(\omega_0)) \end{aligned} \quad (3.6)$$

Which like equation (3.5) uses the fact that $\gamma(\omega) \cong \gamma(\omega_0) + \gamma'(\omega_0)(\omega - \omega_0)$

$\forall \omega \in [\omega_0 - \Delta\omega, \omega_0 + \Delta\omega]$ and the same FT properties.

From equation (3.6) the group time delay of the signal centered at ω_0 is $\gamma'(\omega_0)$ in the envelope of the signal. This is the single entry of the WS time-delay matrix for this simple one-port network given by

$$\begin{aligned}
Q &= \gamma'(\omega) \\
&= j e^{j\gamma(\omega)} (-j) \gamma'(\omega) e^{-j\gamma(\omega)} \\
&= j S^*(\omega) S'(\omega)
\end{aligned} \tag{3.7}$$

Which is simply the time-delay of the outgoing field in the one-port system.

6.2.2 Multi-port System

Let the same network as above have M -ports. Now let the p -th line support an incoming field given by

$$\phi_p^i(w, \omega) = e^{jk(\omega)w} \tag{3.8}$$

Where $1 \leq p \leq M$ and the outgoing field on line m due to the incoming field on line p is given by

$$\phi_p^o(w, m, \omega) = \mathbf{S}_{mp} e^{-jk(\omega)w} = \mathbf{S}_{mp} (\phi_p^i(w, \omega))^* \tag{3.9}$$

The scattering matrix populated by \mathbf{S}_{mp} is both unitary and symmetric.

$$\begin{aligned}
\mathbf{S}^\dagger \mathbf{S} &= \mathbf{I}_M \\
\mathbf{S} &= \mathbf{S}^T
\end{aligned} \tag{6.2}$$

Where \mathbf{I}_M is an $M \times M$ identity matrix.

The outgoing field can be written as

$$\begin{aligned}
\tilde{\phi}_p^o(w, m, t) &= \text{Re} \left\{ \int_{\omega_0 - \Delta\omega}^{\omega_0 + \Delta\omega} A(\omega - \omega_0) \mathbf{S}_{mp}(\omega) e^{j(\omega t - k(\omega)w)} d\omega \right\} \\
&= \text{Re} \left\{ \int_{\omega_0 - \Delta\omega}^{\omega_0 + \Delta\omega} A(\omega - \omega_0) |\mathbf{S}_{mp}(\omega)| e^{-j\gamma_{mp}(\omega)} e^{j(\omega t - k(\omega)w)} d\omega \right\}
\end{aligned}$$

Apply Taylor series expansion to $|\mathbf{S}_{mp}(\omega)| \cong |\mathbf{S}_{mp}(\omega_0)| + |\mathbf{S}_{mp}(\omega_0)|'(\omega - \omega_0)$

$$\begin{aligned}
\tilde{\phi}_p^o(w, m, t) &\cong \text{Re} \left\{ \int_{\omega_0 - \Delta\omega}^{\omega_0 + \Delta\omega} A(\omega - \omega_0) \left(|\mathbf{S}_{mp}(\omega_0)| \right. \right. \\
&\quad \left. \left. + |\mathbf{S}_{mp}(\omega_0)|'(\omega - \omega_0) \right) e^{-j\gamma_{mp}(\omega)} e^{j(\omega t - k(\omega)w)} d\omega \right\} \\
&= \text{Re} \left\{ |\mathbf{S}_{mp}(\omega_0)| \int_{\omega_0 - \Delta\omega}^{\omega_0 + \Delta\omega} A(\omega - \omega_0) e^{-j\gamma_{mp}(\omega)} e^{j(\omega t - k(\omega)w)} d\omega \right. \\
&\quad \left. + \int_{\omega_0 - \Delta\omega}^{\omega_0 + \Delta\omega} A(\omega - \omega_0) |\mathbf{S}_{mp}(\omega_0)|'(\omega - \omega_0) e^{-j\gamma_{mp}(\omega)} e^{j(\omega t - k(\omega)w)} d\omega \right\}
\end{aligned}$$

The first integral is of the same form as the outgoing field in the one-port case. The second integral can be solved by first multiplying by $1 = -j^2$

$$\text{second integral} = \text{Re} \left\{ -j |\mathbf{S}_{mp}(\omega_0)|' \int_{\omega_0 - \Delta\omega}^{\omega_0 + \Delta\omega} j(\omega - \omega_0) A(\omega - \omega_0) e^{-j\gamma_{mp}(\omega)} e^{j(\omega t - k(\omega)w)} d\omega \right\}$$

Now the second integral has the same form as the outgoing field in the one-port system with the additional factor of $j(\omega - \omega_0)$ which results in a time-derivative in the time-domain due to the frequency-shifting property.

$$\begin{aligned}
\tilde{\phi}_p^o(w, m, t) &\cong \text{Re} \left\{ |\mathbf{S}_{mp}(\omega_0)| \int_{\omega_0 - \Delta\omega}^{\omega_0 + \Delta\omega} A(\omega - \omega_0) e^{-j\gamma_{mp}(\omega)} e^{j(\omega t - k(\omega)w)} d\omega \right. \\
&\quad \left. - j|\mathbf{S}_{mp}(\omega_0)|' \int_{\omega_0 - \Delta\omega}^{\omega_0 + \Delta\omega} j(\omega - \omega_0) A(\omega - \omega_0) e^{-j\gamma_{mp}(\omega)} e^{j(\omega t - k(\omega)w)} d\omega \right\} \\
&= |\mathbf{S}_{mp}(\omega_0)| \tilde{A} \left(t - k'(\omega_0)w - \gamma'_{mp}(\omega_0) \right) \cos \left(\omega_0 t - k(\omega_0)w - \gamma_{mp}(\omega_0) \right) \\
&\quad + |\mathbf{S}_{mp}(\omega_0)|' \frac{\partial \tilde{A} \left(t - k'(\omega_0)w - \gamma'_{mp}(\omega_0) \right)}{\partial t} \sin \left(\omega_0 t - k(\omega_0)w - \gamma_{mp}(\omega_0) \right) \\
\tilde{\phi}_p^o(w, m, t) &\cong |\mathbf{S}_{mp}(\omega_0)| \tilde{A} \left(t - k'(\omega_0)w - \gamma'_{mp}(\omega_0) \right) \cos \left(\omega_0 t - k(\omega_0)w - \gamma_{mp}(\omega_0) \right) \\
&\quad + |\mathbf{S}_{mp}(\omega_0)|' \frac{\partial \tilde{A}(t - k'(\omega_0)w)}{\partial t} \sin \left(\omega_0 t - k(\omega_0)w - \gamma_{mp}(\omega_0) \right)
\end{aligned}$$

Since the envelope function $\tilde{A}(t)$ is relatively smooth and narrowband, its time-derivative is small and the second term in the above equation can be ignored.

$$\tilde{\phi}_p^o(w, m, t) \cong |\mathbf{S}_{mp}(\omega_0)| \tilde{A} \left(t - k'(\omega_0)w - \gamma'_{mp}(\omega_0) \right) \cos \left(\omega_0 t - k(\omega_0)w - \gamma_{mp}(\omega_0) \right)$$

As before, the group delay of the outgoing signal is given by $\gamma'_{mp}(\omega_0)$ and therefore

$$\begin{aligned}
q_{mp} &= \gamma'_{mp}(\omega_0) \\
&= j \frac{1}{\mathbf{S}_{mp}(\omega)} \mathbf{S}'_{mp}(\omega)
\end{aligned}$$

Which is, of course, different than demonstrated from the one-port system. In order to reconcile this with equation (4.7), a weighted-average time-delay is defined

$$\langle q_{mp} \rangle = \sum_{m=1}^M |\mathbf{S}_{mp}(\omega)|^2 q_{mp}$$

This quantity is the average time-delay of the field from input port p to all other ports in which each time-delay is weighted by $|\mathbf{S}_{mp}(\omega)|^2$, the fraction of the total field's power delivered from port p to port m . Substituting in q_{mp}

$$\begin{aligned}
\langle q_{mp} \rangle &= j \sum_{m=1}^M |\mathbf{S}_{mp}(\omega)|^2 \frac{1}{\mathbf{S}_{mp}(\omega)} \mathbf{S}'_{mp}(\omega) \\
&= j \sum_{m=1}^M |\mathbf{S}_{mp}(\omega)|^2 \frac{1}{|\mathbf{S}_{mp}(\omega)| e^{-j\gamma_{mp}(\omega)}} \mathbf{S}'_{mp}(\omega) \\
&= j \sum_{m=1}^M |\mathbf{S}_{mp}(\omega)| e^{j\gamma_{mp}(\omega)} \mathbf{S}'_{mp}(\omega)
\end{aligned}$$

$$\begin{aligned}
&= j \sum_{m=1}^M \mathbf{s}_{mp}^*(\omega) \mathbf{s}'_{mp}(\omega) \\
&= \mathbf{Q}_{pp}(\omega)
\end{aligned}$$

Therefore, the diagonal elements of \mathbf{Q} are the average time-delays of the p^{th} incoming field for the multi-port system. There is no direct physical interpretation of the off-diagonal elements, but they remain important.

6.3 WS MODES

6.3.1 Properties of \mathbf{Q}

It turns out that \mathbf{Q} is actually Hermitian as shown by the following

$$\begin{aligned}
\mathbf{Q} &= j\mathbf{S}^\dagger \mathbf{S}' \\
\mathbf{Q}^\dagger &= (j\mathbf{S}^\dagger \mathbf{S}')^\dagger \\
&= -j\mathbf{S}'^\dagger \mathbf{S}
\end{aligned}$$

Taking the derivative with respect to k of equation (6.2) yields a useful relationship

$$\begin{aligned}
(\mathbf{S}^\dagger \mathbf{S})' &= (\mathbf{I}_M)' \\
\mathbf{S}'^\dagger \mathbf{S} + \mathbf{S}^\dagger \mathbf{S}' &= 0 \\
-\mathbf{S}'^\dagger \mathbf{S} &= \mathbf{S}^\dagger \mathbf{S}'
\end{aligned} \tag{6.3}$$

Therefore, it is shown that \mathbf{Q} is Hermitian

$$\begin{aligned}
\mathbf{Q}^\dagger &= j\mathbf{S}'^\dagger \mathbf{S} \\
&= \mathbf{Q}
\end{aligned}$$

And all Hermitian matrices are normal matrices so \mathbf{Q} can be diagonalized such that

$$\mathbf{Q} = \mathbf{W} \bar{\mathbf{Q}} \mathbf{W}^\dagger$$

This is an eigenvalue decomposition of \mathbf{Q} so the column vectors of \mathbf{W} are the eigenvectors of \mathbf{Q} and the diagonal entries of $\bar{\mathbf{Q}}$ are its real-valued eigenvalues. It is a property of Hermitian matrices that their eigenvalues are real-valued. \mathbf{S} can be factorized by \mathbf{W} as follows

$$\mathbf{S} = \mathbf{W}^* \bar{\mathbf{S}} \mathbf{W}^\dagger$$

Substituting the previous two equations into equation (6.1) yields

$$\begin{aligned}
j\mathbf{S}^\dagger \mathbf{S}' &= \mathbf{Q} \\
\mathbf{S}' &= -j(\mathbf{S}^\dagger)^{-1} \mathbf{Q}
\end{aligned}$$

Since \mathbf{S} is unitary, $(\mathbf{S}^\dagger)^{-1} = (\mathbf{S}^\dagger)^*$ and \mathbf{S} is symmetric so $(\mathbf{S}^\dagger)^{-1} = (\mathbf{S}^\dagger)^* = \mathbf{S}^T = \mathbf{S}$ or alternatively, any unitary matrix's inverse is its Hermitian (i.e. complex conjugate transpose) and therefore $(\mathbf{S}^\dagger)^{-1} = \mathbf{S}$. Substituting in the diagonalized forms of \mathbf{S} and \mathbf{Q}

$$\begin{aligned}
\mathbf{S}' &= -j\mathbf{S}\mathbf{Q} \\
&= -j(\mathbf{W}^* \bar{\mathbf{S}} \mathbf{W}^\dagger)(\mathbf{W} \bar{\mathbf{Q}} \mathbf{W}^\dagger)
\end{aligned}$$

$$= -j(\mathbf{W}^* \bar{\mathbf{S}} \mathbf{W}^\dagger)(\mathbf{W} \bar{\mathbf{Q}} \mathbf{W}^\dagger)$$

The matrix, \mathbf{W} , is unitary, therefore $\mathbf{W}^\dagger \mathbf{W} = \mathbf{I}_M$

$$\begin{aligned} \mathbf{S}' &= -j(\mathbf{W}^* \bar{\mathbf{S}} \mathbf{I}_M \bar{\mathbf{Q}} \mathbf{W}^\dagger) \\ &= -j\mathbf{W}^* \bar{\mathbf{S}} \bar{\mathbf{Q}} \mathbf{W}^\dagger \end{aligned}$$

$$\begin{aligned} (\mathbf{S}')^T &= \left(-j(\mathbf{W}^* \bar{\mathbf{S}} \mathbf{I}_M \bar{\mathbf{Q}} \mathbf{W}^\dagger) \right)^T \\ &= -j\mathbf{W}^{\dagger T} \bar{\mathbf{Q}}^T \bar{\mathbf{S}}^T \mathbf{W}^{*T} \\ &= -j\mathbf{W}^* \bar{\mathbf{Q}} \mathbf{S} \mathbf{W}^\dagger \end{aligned}$$

Since \mathbf{S} is symmetric, then $(\mathbf{S}')^T = \mathbf{S}'$ and therefore $\bar{\mathbf{S}} \bar{\mathbf{Q}} = \bar{\mathbf{Q}} \bar{\mathbf{S}}$ so $\bar{\mathbf{S}}$ is a diagonal matrix. The importance of this is illustrated by the following

$$\begin{aligned} \mathbf{Q} &= j\mathbf{S}^\dagger \mathbf{S}' \\ \mathbf{W} \bar{\mathbf{Q}} \mathbf{W}^\dagger &= j\mathbf{S}^\dagger \mathbf{S}' \\ \bar{\mathbf{Q}} &= j\mathbf{W}^\dagger \mathbf{S}^\dagger \mathbf{S}' \mathbf{W} \\ &= j\mathbf{W}^\dagger \mathbf{S}^\dagger \mathbf{W}^* \mathbf{W}^T \mathbf{S}' \mathbf{W} \\ &= j\bar{\mathbf{S}}^\dagger \bar{\mathbf{S}}' \end{aligned}$$

Since the matrices on the left and right sides of the above equation are diagonal, each WS mode corresponding to an entry of $\bar{\mathbf{Q}}$ is uniquely determined by the corresponding entry in $\bar{\mathbf{S}}^\dagger$ and $\bar{\mathbf{S}}'$ thus it can be said that the WS modes are entirely decoupled from one another and the entries of $\bar{\mathbf{Q}}$ entirely characterize the time delays of the system.

6.3.2 What does $\bar{\mathbf{Q}}$ represent?

From the multi-port system analysis in section 6.2.2, it is well established that the diagonal entries of \mathbf{Q} correspond to the average time-delay experienced by the incoming wave in port p exiting from all ports. The diagonal elements of $\bar{\mathbf{Q}}$ correspond to time delays as well, but not in the same sense. The WS modes described by the eigenvectors and eigenvalues of \mathbf{Q} each provide a unique set of incoming waves (eigenvectors; columns of \mathbf{W}) to all ports of the system such that all outgoing waves from all ports exit the system with the same exact time delay (eigenvalue; diagonal entries of $\bar{\mathbf{Q}}$).

6.3.3 Fields of WS Modes

As mentioned in the previous section, the q^{th} -column of \mathbf{W} provides a set of weights that when multiplied by their corresponding incoming waves, provide a total incoming wave of the q^{th} WS mode. More formally, if the $\mathbf{Q}(\omega_0)$ matrix at a frequency ω_0 is obtained and diagonalized with the methods shown above providing the eigenvectors in $\mathbf{W}(\omega_0)$, then

$$\phi_{WS,q}^i(w, \omega_0) = \sum_{p=1}^M \mathbf{w}_{pq}(\omega_0) \phi_p^i(w, \omega_0)$$

Is the total incoming wave of the q^{th} WS mode. When the system is excited with $\phi_{WS,q}^i(w, \omega_0)$, then the outgoing wave $\phi_{WS,q}^o(w, \omega_0)$ dwells in the system for the exact amount of seconds given by the corresponding eigenvalue in $\mathbf{Q}_{qq}(\omega_0)$.

6.3.4 WS and Method of Moments

If the incoming wave generated based on WS modes is used in a method of moments code, the corresponding sources can be solved for as in a traditional solve using any valid integral equation with the following steps

- 1) Compute \mathbf{Q} for geometry of interest making sure to use enough harmonics for scattering matrix
- 2) Diagonalize \mathbf{Q}
- 3) Create new incident field from q -th column of \mathbf{W}
- 4) Use new incident field to fill the RHS when solving the desired integral equation

\mathbf{Q} can be computed directly or indirectly.

Indirect calculation of \mathbf{Q}

$$\mathbf{Q} = j\mathbf{S}^\dagger \mathbf{S}'$$

Direct calculation

$$\mathbf{Q} = \frac{-1}{2k} \mathbf{J}_s^\dagger \mathbf{V}_s' + \frac{1}{2k^2} \mathbf{J}_s^\dagger \text{Re}\{\mathbf{Z} + k\mathbf{Z}'\} \mathbf{J}_s + \frac{j}{8k^2} \mathbf{J}_s^\dagger (\mathbf{V}_s^* \mathbf{V}_s'^T - \mathbf{V}_s'^* \mathbf{V}_s^T) \mathbf{J}_s$$

7 ADAPTIVE CROSS APPROXIMATION

The adaptive cross approximation (ACA) is a general-purpose algorithm for compressing low rank matrices into two matrices that when multiplied with matrix multiplication approximate the original matrix. “General-purpose” meaning that the algorithm is agnostic to the context of the matrix or the mathematical functions generating the matrix. This makes it easy to implement and convenient for general codes such as mine where I have multiple integral equation options. As implemented in the code, ACA allows for simple swapping of the function generating the matrix entries used in the ACA routine to change integral equations. ACA compression of the \mathbf{Z} matrix can be used in all integral equation solvers as well as in computing the scattering matrix.

7.1 ALGORITHM

Let $\mathbf{Z}^{m \times n}$ be a sub-matrix of the total \mathbf{Z} matrix encapsulating interactions between two well separated groups of elements in a MoM formulation. The goal of ACA is to approximate this matrix by the matrix $\tilde{\mathbf{Z}}^{m \times n}$ which is decomposed into two matrices, $\mathbf{U}^{m \times r}$ and $\mathbf{V}^{r \times n}$ such that

$$\tilde{\mathbf{Z}}^{m \times n} = \mathbf{U}^{m \times r} \mathbf{V}^{r \times n}$$

Where r is the rank of $\mathbf{Z}^{m \times n}$. The objective of the following ACA algorithm is to minimize the error between $\mathbf{Z}^{m \times n}$ and $\tilde{\mathbf{Z}}^{m \times n}$ given by

$$\|\mathbf{R}^{m \times n}\| = \|\mathbf{Z}^{m \times n} - \tilde{\mathbf{Z}}^{m \times n}\| \leq \epsilon \|\mathbf{Z}^{m \times n}\|$$

Where $\|\mathbf{A}\| = \sqrt{\sum_{i=1}^m \sum_{j=1}^n |a_{ij}|^2}$ is the Frobenius norm, ϵ is an arbitrary tolerance and $\mathbf{R}^{m \times n}$ is the error matrix.

The exact implementation of ACA used in my code is outlined in “The Adaptive Cross Approximation Algorithm for Accelerated Method of Moments Computations of EMC Problems” by Zhao et al.

7.2 METRICS

Insight into the performance of the ACA algorithm can be predicted with an understanding of key metrics describing the approximation. Compression ratio, the number of elements per node and the rank of compressed matrices are such metrics.

Compression Ratio

The compression ratio is defined as the total number of elements stored across all sub- \mathbf{Z} matrices used in the ACA solver whether compressed or uncompressed divided by the total number of matrix elements stored in the full \mathbf{Z} matrix used in the direct solver. The compression ratio shows approximately how much memory is saved and how many fewer multiplications are needed in the ACA solver. This metric will be less than 1 when an ACA solver outperforms a traditional solver and is probably the most insightful metric computed in my code. Note that if a few matrices are heavily compressed, but most node-to-node interactions are uncompressible, then the compression ratio will remain high. It is also useful to store the percentage of sub- \mathbf{Z} matrices that were compressed since this information is ignored in compression ratio.

Elements Per Node

The second most useful metric is the number of elements per node. My code computes the average, minimum and maximum across all non-empty nodes of the octree. Correlating the average number of elements per node with compression ratio will help build intuition on the size of the octree and expected performance of the ACA solver when compared with the traditional solver.

Matrix Rank

The average, minimum and maximum rank of compressed matrices is saved. In combination with the number of elements per node, this is useful. A low average rank compared to the average number of elements per node means there is a lot of compression going on. This information does not suffer from an effect akin to uncompressed matrices raising the compression ratio.

8 APPENDIX EQUATION SECTION (NEXT)

8.1 LINEAR ALGEBRA

8.1.1 Matrix Diagonalization

A diagonal matrix \mathbf{A} is a square matrix for which

$$\mathbf{P}^{-1}\mathbf{A}\mathbf{P} = \mathbf{D} \text{ or equivalently } \mathbf{A} = \mathbf{P}\mathbf{D}\mathbf{P}^{-1} \quad (8.1)$$

Where \mathbf{D} is a diagonal matrix of the eigenvalues of \mathbf{A} and the columns of \mathbf{P} are the eigenvectors of \mathbf{A} .

In the case that \mathbf{A} is also self-adjoint ($\mathbf{A} = \mathbf{A}^\dagger$), then equation **Error! Reference source not found.** becomes

$$\mathbf{A} = \mathbf{P}\mathbf{D}\mathbf{P}^\dagger \quad (4.1)$$

9 REFERENCES

- K. Zhao, M. N. Vouvakis, and J.-F. Lee, "The adaptive cross approximation algorithm for accelerated method of moments computations of emc problems," *IEEE Transactions on Electromagnetic Compatibility*, vol. 47, no. 4, pp. 763–773, 2005.
- D. Wilton, S. Rao, A. Glisson, D. Schaubert, O. Al-Bundak, and C. Butler, "Potential integrals for uniform and linear source distributions on polygonal and polyhedral domains," *IEEE Transactions on Antennas and Propagation*, vol. 32, no. 3, pp. 276–281, 1984.
- A. J. Burton and G. F. Miller, "The application of integral equation methods to the numerical solution of some exterior boundary-value problems," *Proceedings of the Royal Society of London. A. Mathematical and Physical Sciences*, vol. 323, no. 1553, pp. 201–210, 1971.
- U. R. Patel and E. Michielssen, "Wigner–Smith time-delay matrix for Electromagnetics: Theory and phenomenology," *IEEE Transactions on Antennas and Propagation*, vol. 69, no. 2, pp. 902–917, 2021.
- Much of this work comes from discussions with and the notes of Utkarsh Patel and Eric Michielssen at the University of Michigan.